Converging Topographic Axes of Connectivity and Genetic Architectures Scaffold Cortical Patterning

Short title: Connectopies scaffold cortical patterning underpinned by genetic gradients

Deying Li[1,3], Liang Ma[1,3], Yufan Wang[1,3], Yuheng Lu[1,3], Haiyan Wang[1,3], Yaping Wang[1,2,3], Chaohong Gao[1,2,3], Luqi Cheng[4], Yu Zhang[5], Zhengyi Yang[1,2,3], Simon B Eickhoff[6,7], Chi-Hua Chen[8], Congying Chu[1,3*], Lingzhong Fan [1,2,3,9,10*]

[1] Brainnetome Center, Institute of Automation, Chinese Academy of Sciences, 100190, Beijing, China

[2] Sino-Danish Center, [3] University of Chinese Academy of Sciences, 100190, Beijing, China.

[4] School of Life and Environmental Sciences, Guilin University of Electronic Technology, Guilin 541004, China

[5] Research Center for Augmented Intelligence, Zhejiang Lab, 311100, Hangzhou, Zhejiang, China.

[6] Institute of Neuroscience and Medicine (INM-7: Brain and Behaviour), Research Centre Jülich, 52425 Jülich, Germany.

[7] Institute of Systems Neuroscience, Heinrich Heine University Düsseldorf, 40225 Düsseldorf, Germany.

[8] Department of Radiology, University of California San Diego, La Jolla, CA 92093

[9] CAS Center for Excellence in Brain Science and Intelligence Technology, Institute of Automation, Chinese Academy of Sciences, 100190, Beijing, China

[10] School of Health and Life Sciences, University of Health and Rehabilitation Sciences, 266000, Qingdao, Shandong, China

***Corresponding Authors**:

Lingzhong Fan, Institute of Automation, Chinese Academy of Sciences, Beijing 100190, China. Email: lingzhong.fan@ia.ac.cn, Phone: 010 -8254 4523

or Congying Chu, Institute of Automation, Chinese Academy of Sciences, Beijing 100190, China. Email: congying.chu@ia.ac.cn, Phone: 010 -8254 4770

Abstract

Genetic factors have involved the gradual emergence of cortical areas since the neural tube begins to form, shaping the specialization of neural circuits in the human brain. Informed by invasive tract-tracing measurements, the cortex exhibits marked interareal variation in connectivity profiles, yet how this spatial variation is encoded in genetics remains unclear. Instead of considering a complex one-to-one mapping between genetic coding and interareal connectivity variation, we hypothesized the existence of a more efficient way that the organizing principles are embedded in genetic profiles to underpin the configuration of connectivity across the human cortex. Specifically, we found that a noninvasive neuroimaging measure, i.e., global connectopy derived from diffusion-weighted MRI tractography, reliably indexes the organizing principles of interareal connectivity variation, and it captures three dominant topographic patterns along the dorsoventral, rostrocaudal, and mediolateral axes of the cortex. We further found that the global connectopies converge to the gradients of vertex-by-vertex genetic correlation matrix on the phenotype of cortical morphology and the cortex-wide spatiomolecular gradients. Moreover, we found the critical role of genes related to brain morphogenesis in scaffolding the global connectopies. Our findings identify a common space linking genetic profilings and interareal connectivity variation, which may contribute to the accurate formation of cortical connections and arealization.

Introduction

Mounting evidence has suggested that the genetic effects on the anatomical phenotypes of the human brain are spatially heterogeneous [1-5], demonstrating the vital roles of genes in establishing the configuration of brain space, such as the anatomical hierarchy [6] and the wiring diagram [7-9]. Especially the pattern of brain wiring that can be characterized by using neuroimaging-based tractography is a reliable source to indicate the process of cortical arealization [10,11], reflecting the differentiation in local microstructures and connectivity profiles. The interareal connectivity variation has further revealed the spatially heterogeneous patterns of cortical organization, such as the regional controllability related to cognitive dynamics [12-14]. In contrast, the deficit of interareal connectivity has demonstrated the specificity to the behavioral manifestations of the brain lesion [15,16]. However, unifying principles for the spatial heterogeneity embedded in both genetic topography and interareal connectivity variation are still largely unknown.

The spatiotemporal distribution of genetic factors along the developing brain is found to set the primary coordinates for various developmental processes, including axonal guidance, cortical patterning, and regional identity [17-20]. The gene-coded signaling molecules and transcription factors expressed in graded concentrations throughout the cortex are ontogenetically conserved to maturity [21,22], indicating an initial rule of brain wiring. Specifically, under the effect of morphogens secreted in the patterning centers, transcription factors are expressed in a graded manner and determine the areal fate and the expression of cell-surface molecules, thus determining the topographic organization of synaptic inputs and outputs [1,23] and directing axonal outgrowth [24]. Nevertheless, considering the complexity and specificity of neural circuits, it would be difficult to conceive the existence of a genetic code capable of unambiguously generating the wiring patterns [25]. Alternatively, genetics may efficiently code simple pattern formation rules underpinning the construction of neural circuits [25]. Therefore, we further hypothesized that the pattern-based rules coded by genetics could be represented by the spatially distributed gene profiles to characterize the spatial heterogeneity embedded in genetic topography. Recent advances in acquiring high-throughput transcriptomic data of the human brain [26] and large-scale twin samples [2,3] with neuroimaging data provide essential resources to test our hypothesis.

Furthermore, even if we could identify the genetic topography accounting for the cortical

heterogeneity, we would still need to verify whether we could leverage it to unify the interareal connectivity variation. Recent studies revealed that cortical areas are hierarchically along the cortex from a large-scale gradient perspective of connectivity [27,28], indicating that the cortex is organized topologically within interareal connectivity variation. However, traditional neural circuit tracing techniques, including classical tracers or virus tracing, are precluded in humans, thereby creating the need for noninvasive measures of the topography embedded in interareal connectivity variation, which would contribute to testing the existence of unified rules underlying the genetic topography and interareal connectivity variation.

To address these open questions, we combined diffusion tractography with a dimension reduction framework and revealed three overlapping modes of fine-grained white-matter organization. The three global connectopies separately run along the dorsoventral, rostrocaudal, and mediolateral axes, formed by gradual shifts in connectivity driven by specific tracts, which we mapped to distinct modes of function. Similar to the first axis, the other two connectivity axes were not constrained a priori to follow any spatial organization of the brain (e.g., spatial coordinates, cytoarchitecture, or macroscale anatomy) but instead were allowed to reveal how the anatomical and axial alignments are embedded in the intrinsic structure of transcriptional variation. We then explored how the three axes are biologically and developmentally distinct and demonstrated that they constrained the cortical patterning and could be used to explain most of the spatial variation across key anatomical and functional brain maps derived from neuroimaging. Moreover, we demonstrated a correspondence between the genetic influence on cortical morphology and the global connectopies and identified genes associated with the global connectopies that are also involved with brain morphogenesis. We further established that the three global connectopies are consistent with morphogen gradients in the developing brain and spatiomolecular gradients in adulthood and provided evidence that specific genes drive the formation of the cortical organization. Finally, we identified specific white matter tracts that serve as the scaffold for the global connectopies. The current study highlights the significance of structural connections as the foundation of brain function and provides essential insights into the topographic principles of brain organization.

Materials and Methods

Data and preprocessing

Data collection We used a publicly available dataset containing 100 unrelated subjects (HCP-U100) (54 females; mean age, 29.11±3.67; age range, 22-36) provided by the Human Connectome Project (HCP) database [29] (http://www.humanconnectome.org). All the scans and data from the individuals included in the study had passed the HCP quality control and assurance standards.

The scanning procedures and acquisition parameters were detailed in previous publications [30]. In brief, T1w images were acquired with a 3D MPRAGE sequence on a Siemens 3T Skyra scanner equipped with a 32-channel head coil with the following parameters: TR = 2400 ms, TE = 2.14 ms, flip angle = 8°, FOV = 224×320 mm^2, voxel size = 0.7 mm isotropic. Diffusion data were acquired using single-shot 2D spin-echo multiband echo planar imaging on a Siemens 3 Tesla Skyra system (TR = 5520 ms, TE = 89.5 ms, flip angle = 78°, FOV = 210×180 mm). These consisted of three shells (b-values = 1000, 2000, and 3000 s/mm^2), with 90 diffusion directions isotropically distributed among each shell and six b = 0 acquisitions within each shell, with a spatial resolution of 1.25 mm isotropic voxels.

Image preprocessing The human T1w structural data had been preprocessed following the HCP's minimal preprocessing pipeline [30]. In brief, the processing pipeline included imaging alignment to standard volume space using FSL, automatic anatomical surface reconstruction using FreeSurfer, and registration to a group average surface template space using the multi-modal surface matching (MSM) algorithm [31]. Human volume data were registered to Montreal Neurological Institute (MNI) standard space, and surface data were transformed into surface template space (fs_LR).

The diffusion Images were processed using FDT (FMRIB's Diffusion Toolbox) of FSL. The main steps are normalization of the b0 image intensity across runs and correction for echo-planar imaging (EPI) susceptibility, eddy-current-induced distortions, gradient-nonlinearities, and subject motion. DTIFIT was then used to fit a diffusion tensor model. The probability distributions of the fiber orientation distribution were estimated using Bedpostx.

Next, skull-stripped T1-weighted images for each subject were co-registered to the subject's b0 images using FSL's FLIRT algorithm. Then nonlinear transformations between the T1 image and the MNI structural template were obtained using FSL's FNIRT. Based on concatenating these, we

derived bi-directional transformations between the diffusion and MNI spaces.

Parcellation approach The above main analyses were vertex-wise, but other gradients and modalities of specific data were only available with specific parcellations. Specifically, DK-308, a sub-parcellation of the DK atlas with 308 equally sized ROIs of 500 mm^2 each [32], had been parcellated by Von Economo cytoarchitectonics; neurotransmitter data were only available with a Schaefer-400 parcellation [33], which combined local gradient and global similarity approaches via gradient-weighted Markov random models; HCP multi-modal parcellation (HCP-MMP) [34] was also utilized for discovery and replication. HCP-MMP, which has been widely used, was generated using a gradient-based parcellation approach with similar gradient ridges presenting in roughly corresponding locations in both hemispheres.

Connectopy mapping

Tractography and connectivity fingerprints To map the whole-brain connectivity pattern, we performed probabilistic tractography using FSL's probtrackx2 accelerated by using GPUs [35,36]. Specifically, the white surface was set as a seed region tracking to the rest of the brain with the ventricles removed and down-sampled to 3 mm resolution. The pial surface was used as a stop mask to prevent streamlines from crossing sulci. Each vertex was sampled 5000 times (5000 trackings) based on the orientation probability model for each voxel, with a curvature threshold of 0.2, a step length of 0.5 mm, and a number of steps of 3200. This resulted in a (*whole-surface vertices*) × (*whole-brain voxels*) matrix for further analysis.

We created connectivity fingerprints following the pipeline in [37]. Specifically, we first reconstructed 72 fiber bundles using a pre-trained deep-learning model, TractSeg [38], and down-sampled the resulting tract masks to 3 mm resolution, yielding a (*tracts*) × (*whole-brain voxels*) matrix. Then the connectivity fingerprints were generated by the product of this tract matrix, and the whole-brain connectivity matrix was obtained as described in the Tractography section and normalized. The columns of the resulting (*tracts*) × (*whole-surface vertices*) matrix showed the connectivity distribution pattern of each cortical vertex, while the rows revealed the cortical termination patterns of the tracts.

Tractogram covariance analysis We calculated the tractogram covariance (TC) matrix to characterize the structural connectivity similarity profile. The vertex profiles underwent pairwise

Pearson correlations, controlling for the average whole-cortex profile. For a given pair of vertices, *I* and *j,* TC was calculated as

$$TC(i,j) = \frac{r_{ij} - r_{ic}r_{jc}}{\sqrt{(1 - r_{ic}^2)(1 - r_{jc}^2)}}$$

in which r_{ij} was the Pearson correlation coefficient of the structural connectivity profile at vertices *I* and *j*, r_{ic} the correlation of the structural connectivity profile at vertex *I* with the average connectivity profile across the whole cortex, and r_{jc} the correlation of the structural connectivity profile at vertex *j* with the average connectivity profile across the entire cortex. A symmetric ~30k×30k TC matrix was produced for each subject. Then, the TC matrices of all subjects were averaged separately for the left and right hemispheres to get a group-level TC matrix for each hemisphere. In line with a previous study [39], the TC matrix was proportionally thresholded at 90% per row, with elements above zero retained to remove negative connections.

Connectopy decomposition The TC matrix was transformed into a non-negative square symmetric affinity matrix using a cosine affinity kernel. Then diffusion map embedding was implemented to identify the principal gradient components [40]. Diffusion map embedding is a nonlinear manifold learning technique that maps cortical and cerebellar gradients [28,41]. Along these gradients, cortical vertices with similar connectivity profiles are embedded along the axis. Diffusion map embedding is relatively robust to noise and less computationally expensive than other nonlinear manifold learning techniques.

Global connectopies were computed separately for the left and right hemispheres with two key parameters: α controls the influence of the density of sampling points on the manifold, and t controls the scale of the eigenvalues. Here we set α=0.5 and t=0 as recommended [28]. The amount of explained variance was assessed, and the first three global connectopies were chosen to map onto the cortical surface for further analysis. To discover whether low-dimensional connectivity fingerprints could capture most of the structural connectivity information, we also generated global connectopies based on these connectivity fingerprints using the same methods.

Visualization of connectopies To inspect the global connectopies together intuitively, we plotted every two global connectopies in a 2D space and assigned them colors based on their positions. Then we generated RGB values for each vertex by normalizing three global connectopy values and mapped them on the surface, showing the dominant global connectopy at the vertex. Specifically,

for the first gradient, values of all vertices were normalized from zero to one, resulting in a value of the red channel. The other two were conducted the same.

Relation to biological features To further validate the biological basis of the global connectopies, we mapped their distributions on atlases of laminar differentiation and cytoarchitectural classes. To this end, each vertex was assigned to one of four levels of laminar differentiation (i.e., idiotypic, unimodal, heteromodal, or paralimbic) based on the model of [42] and one of the seven Von Economo/Koskinas cytoarchitectural classes (i.e., primary sensory, secondary sensory, motor, association 1, association 2, limbic, or insular) [43].

For the laminar differentiation maps, we referred to the map provided by [44]. For the cytoarchitectural classes, Vertes et al. subdivided the DK atlas into 308 equal-sized ROIs of 500 mm^2 and assigned each region to one of the seven cytoarchitectural types according to the laminar structure of the cortex [32], with five types delineated by von Economo, that is, the primary motor cortex/precentral gyrus, two types association cortices, and secondary and primary sensory areas along with two additional subtypes: the limbic cortex (including the entorhinal, retrosplenial, presubicular and cingulate cortices, and thus primarily constitutes the allocortex) and the insular cortex. We then estimated the situation of each class along the global connectopy by the correspondence between the global connectopy value and the vertex class.

NeuroSynth term-based meta-analysis We projected the meta-analytical task-based activation along the global connectopies to investigate the association between functional decoding and our global connectopies. Here, we chose 590 terms related to specific cognitive processes that had been selected in previous publications (the full list of terms can be found in [45]). The activation maps for the 590 cognitive terms were downloaded from the NeuroSynth database (https://neurosynth.org/). We generated 20 binarized masks at five-percentile increments of the global connectopy. Each of these 20 maps ranging from 0-5% to 95%-100%, were used as inputs to the subsequent meta-analysis. Each function term had a mean activation z-score per bin. Terms included in the visualization were those that had the highest two z-scores in each bin. A significance threshold of $z > 0.5$ was added as a visualization constraint.

Comparison to function-related gradients To compare the gradient maps, we estimated the correspondence of these gradient maps to our global connectopies using Spearman rank correlation. Most of the gradient maps were derived from the neuromaps distribution [46]. Gradients of histology

and microstructural profile covariance had also been computed previously [39], and the gradients of the neurotransmitters were from [47]. Finally, we characterized the gradient of axon density based on the number of axons [48]. Notably, the maps were obtained in their original coordinate system, so we converted them all to fsaverage_LR32k space. Permutation tests (10000 times) were used to assess statistical significance.

Note that the neurotransmitter data were only available for the "Schaefer-400" parcellation scheme before computing the correlation. Each parcel was assigned to the mean connectopy value across the vertices in the parcel, as in the other gradient maps.

Hierarchical organization analysis

We implemented hierarchical clustering using global connectopies to test our hypothesis that global connectopies could guide the parcellation across the whole cortex. At the first level, the vertices were sorted in descending order from the first global connectopy. Brain regions were partitioned into two subregions based on the sign of the connectopy value. Furthermore, based on the positivity and negativity of the second and third global connectopies, the whole cortex was partitioned into eight modules.

Gene analysis

Genetic correlation analysis of thickness and surface area We selected 194 twins from the HCP database (102 monozygotic and 92 dizygotic pairs; mean age, 29.96±2.96; age range, 22-36). The cortical surface was reconstructed to measure the cortical thickness and surface areas at each surface location using FreeSurfer in the fsaverage3 template to reduce computation time.

In a classical twin study of sets of MZ and DZ twins, four latent factors could account for the variance of any phenotype: additive genetic effects (A); non-additive genetic effects, including dominance (D); common or shared environmental effects (C); and non-shared or individual-specific environmental effects [49]. Because of the minimal difference between the A and D effects, we fitted bivariate ACE models to compute the genetic correlations of the cortical thickness and surface area between two vertices of the cortex. Thus, the genetic covariance was calculated decomposed from the total phenotypic correlation. The analyses were performed using OpenMx [50].

Then we implemented diffusion map embedding on the genetic correlation matrix and

compared it with the global connectopies. Genetic patterning results were obtained from previous studies [1,2], which parcellated the cortex into four and twelve clusters. The parcellation results were compared with the modules derived from hierarchical clustering using the global connectopies.

AHBA data and preprocessing Regional microarray gene expression data were obtained from 6 postmortem brains (1 female, ages 24-57) provided by the Allen Human Brain Atlas (AHBA, https://human.brain-map.org). The data were processed using the abagen toolbox (version 0.1.1; https://github.com/rmarkello/abagen) [51]. First, the microarray probes were reannotated [52], and the probes that did not match a valid Entrez ID were excluded. Then, the probes were filtered based on their expression intensity relative to background noise, and the probes with the maximum summed adjacency for representing the corresponding gene expression were kept, yielding 15633 genes that corresponded to more than one probe. Last, we resampled the output gene expression map in fs5 space to fsaverage_LR32k space for subsequent study.

Gene enrichment analysis We used a prediction framework, partial least squares regression (PLSR), to determine the covariance between gene expression and global connectopies. Then we conducted 1000 bootstrapping to estimate the error of the weight of each gene. The normalized weight of each gene was denoted as the weight divided by the estimated error [53].

Genes were selected as the top and bottom 0.83% genes (n = 260) of each global connectopy's gene list, corrected for both tails and all three global connectopies for multiple comparisons. Each gene set combining both tails underwent gene ontology enrichment analyses. Gene sets that extended across the three global connectopies were also submitted to the analysis. ToppGene (https://toppgene.cchmc.org), which contains the whole list of AHBA genes as the background gene set, was used to conduct the analysis. The following term categories were assessed: GO: Molecular Function, GO: Biological Process, GO: Cellular Component, Pathway, and Disease.

We collected gene expression data for all time points in the BrainSpan dataset to determine the developmental pattern of gene expression. Only genes associated with all three global connectopies were selected. Non-negative matrix factorization was used to derive the gene expression components for each macrostructure in the brain.

Global connectopy related gene analysis We further selected genes expressing the same pattern as any of the three global connectopies in AHBA [54]. Each global connectopy was subdivided equally into eight parts, and two sample t-test was used to assess the difference of gene expression of

selected genes between the first and the last cluster [55].

Correspondence to spatiomolecular gradients Researchers recently reported three spatiomolecular gradients that retained the same pattern as morphogenetic gradients during their development. These gradients varied along three spatially embedded axes [22]. We only used data from the left hemisphere because few samples in the AHBA were obtained from the right hemisphere. We replicated these molecular gradients at the ROI level with the "Schaefer-400" parcellation scheme and explored the correlation with the three global connectopies in this study.

Projection onto the white matter

Projection of the global connectopies onto the white matter voxels To project our global connectopies onto the white matter, we assigned the connectopy value of the vertex, which had the strongest connection strength measured by the tractography, to each white matter voxel. The same procedure was also conducted on the global connectopies space, and the three global connectopies were shown together.

We also used general linear models (GLM) to assess this relationship. Specifically, we used the gradient component as an independent variable and the structural connection matrix as a dependent variable. Note that the structural connection of each subject was obtained from probabilistic tractography in individual diffusion space. We registered each to MNI standard space and averaged, resulting in a group-level structural connection matrix.

Projection of the connectopies onto the white matter tracts To investigate how the global connectopies are related to the underlying white matter tracts, we made a tract projection map using the tract mask generated by TractSeg. Seventy-two tracts identified by TractSeg were grouped into five types for analysis: association tracts, commissural tracts, projection tracts, thalamo tracts, and striato tracts (Table S1). The mean value and variance of the voxels in the tract were calculated to reveal the relationship between the tracts and global connectopies.

Results

Three global connectopies in the human brain

To explore how the spatial organization of the human brain is shaped by the underlying structural connections with the white matter, we characterized the global connectopies across the whole brain (Figure 1a, left). We first built a vertex-wise structural connectivity similarity profile matrix using 100 unrelated subjects from the Human Connectome Project dataset. Specifically, structural connectivity profiles were obtained from probabilistic tractography along ~30k vertices for each hemisphere and were correlated between each pair of vertices. Tractogram covariance (TC) matrices were thresholded at 0 and averaged across subjects. In short, the TC matrix captured structural connectivity similarity across the whole brain.

We implemented diffusion embedding on the TC matrix, a manifold learning method previously used to capture functional gradients. The resultant components revealed the position of vertices along the axes that had the most dominant differences in the given structural connectivity profile. The first three global connectopies separately showed dorsoventral, rostrocaudal, and mediolateral patterns (Figure 1b) and together accounted for 33% of the total variance (Figure 1a, right). These patterns were stable regardless of the number of subjects considered (Figure S1, 2).

More specifically, the first global connectopy (Global connectopy 1 dorsoventral, GC1-DV), following a dorsoventral pattern, was anchored on one end by the occipital, inferior temporal, and orbital frontal cortex and on the other end by the motor and sensorimotor cortex. The second global connectopy (Global connectopy 2 rostrocaudal, GC2-RC) varied along a rostrocaudal axis, radiating from the occipitoparietal cortex and ending in the prefrontal cortex. The third global connectopy (Global connectopy 3 mediolateral, GC3-ML) showed a mediolateral pattern, with the highest expression in the lateral temporal and prefrontal cortex and the lowest in the cingulate cortex (Figure 1b).

To investigate whether these global connectopies recapitulated the biological basis of the brain organization, we mapped the distribution of these global connectopies according to their laminar differentiation and cytoarchitecture classes. The idiotypic regions identified by laminar differentiation revealed two extremes in the GC1-DV, with the dorsal end corresponding to the primary second sensory cortices in terms of cytoarchitecture classification and the ventral end

affiliated with the primary motor network (Figure S5, 6) and corresponding to the visual network and sensorimotor network in terms of Yeo's intrinsic functional network [56]. Most of the idiotypic regions and the areas of unimodal cortex were located in the posterior extreme of the GC2-RC, and the cingulate cortex, part of the limbic network, varied broadly along the global connectopy by the "anterior-posterior" pattern of the global connectopy (Figure S5). The medial part of the GC3-ML occupied the paralimbic cortex, while the lateral part was primarily situated in the association cortex, or heteromodal cortex (Figure S5). These differences demonstrated the cytoarchitectural distinctiveness in the regions at the extremes of the global connectopies.

Note that different regions along the global connectopies belong to distinct intrinsic functional networks. We thought that these affiliations might involve different cognitive functions, so we conducted a meta-analysis to investigate this relationship. The ventral end of GC1-DV is characterized by a visual network that includes "navigation," "episodic," and "faces." In contrast, the dorsal end is characterized by terms about sense and movement, such as "limb," "foot," and "finger" (Figure 1c, left). In GC2-RC, we observed a focus on multisensory and motion terms anteriorly and on "tactile" and "finger" processing posteriorly (Figure 1c, middle). GC3-ML was related to "autobiographical," "craving," and "gestures" in medial regions and to "competing," "risking," and "sentences" in lateral regions (Figure 1c, right).

We also collected a selection of gradient maps from neuromaps [46] and other public studies [47] and made a comparison with the global connectopies (Figure S7). We found that GC1-DV was correlated with the second functional gradient captured by functional connectivity (r = -0.64, p < .0001), which differentiates regions within the unimodal cortex, whereas GC2-RC showed correlation with the first functional gradient (r = -0.49, p < .0001). Notably, the global connectopies showed high correlations with MEG recording maps, including the alpha, beta, delta, gamma, and theta bands ($r_{\text{GC1-DV, beta}}$ = 0.91, $r_{\text{GC1-DV, theta}}$ = 0.62, $r_{\text{GC2-RC, delta}}$ = -0.64, $r_{\text{GC2-RC, gamma1}}$ = -0.62, $r_{\text{GC2-RC, gamma2}}$ = -0.52, $r_{\text{GC2-RC, theta}}$ = -0.51, all p < .0001, Figure S7). Supporting the view that the underlying brain structure is fundamental to the functions across the brain, we think that our findings may provide greater insight into the relationship between microscale structural and macroscale functional features of the cortex.

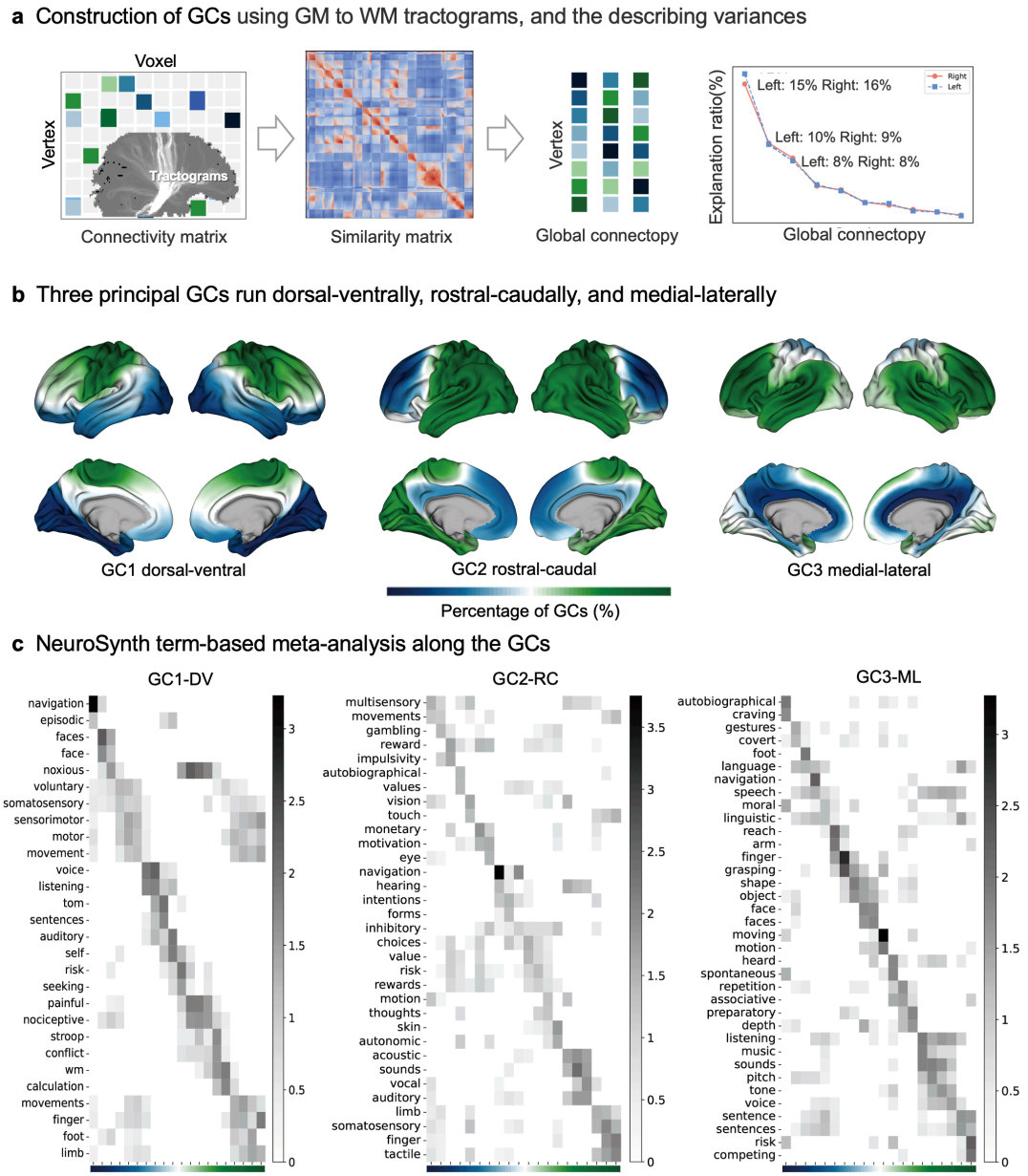

Figure 1. Three global connectopies in the human cerebral cortex. (a) The construction of global connectopies. White matter tractograms were calculated to get a similarity matrix, i.e., a tractogram covariance (TC) matrix. Diffusion embedding was implemented on the TC matrix, resulting in low-dimensional gradients. A scree plot describing variance is shown on the right. **(b)** The first three global connectopies ran dorsoventrally, rostrocaudally, and mediolaterally and were termed GC1-DV, GC2-RC, and GC3-ML, respectively. **(c)** NeuroSynth term-based meta-analysis along the global connectopies. Terms that had the highest two z-scores for each binarized mask of the global connectopies were included in this visualization.

Global connectopies guide the process of arealization

To inspect the global connectopies as a unit, we normalized three connectopy values at each vertex to generate RGB values and mapped them on the surface to make lobes or subregions seen distinctly (Figure 2a). We termed this map, which quantified the topography of the dominant global connectopy, the global connectopic space. The cortex, shown in red, green, and blue, indicated the individual regions that were dominated by each global connectopy. The regions that were dominated by a combination of more than one global connectopy were done in different colors, e.g., the "yellow" region was dominated by the first and second global connectopies together, as shown in the cube in Figure 2a. We plotted every pair of global connectopies in a 2D space and assigned colors based on their unique positions. When these were propagated to the surface, the first and the second global connectopies interacted to split the whole brain into the prefrontal cortex and limbic cortex, sensorimotor and motor cortex, and occipitotemporal cortex (Figure 2b). Similarly, the frontal cortex, limbic cortex, and occipitotemporal cortex were shown when the first and the third global connectopies were considered together, and the prefrontal cortex, limbic cortex, and others were shown when the second and the third connectopy were combined (Figure 2b).

Since the global connectopies characterized the spatial organization across the whole brain, we hypothesized that these global connectopies could shape the process of arealization. So, we then partitioned the brain by hierarchical clustering using the three global connectopies (Figure 2c). At the first level, the brain was partitioned into two modules based on the positive and negative signs of the first global connectopy. These two modules coincided with the division between the dorsal and ventral brain regions. Each module was further partitioned into two modules at each level by the sign of the global connectopies. The rostrocaudal and mediolateral patterns emerged after the corresponding global connectopy was considered. In the end, eight modules were captured. These were the ventral and dorsal somatomotor cortex, lateral prefrontal cortex, cingulate gyrus, lateral temporal cortex + angular gyrus, medial occipital cortex + occipital polar cortex, orbitofrontal cortex, and ventromedial prefrontal cortex + posterior cingulate cortex (Figure 2c).

We found that both the four-module and eight-module divisions showed overlap with one of the classes of laminar, cytoarchitecture, and genetic patterning and thus were consistent with brain areas defined by histology or a hereditary pattern. We concluded that the global connectopies

captured most of the structural connectivity information of the brain, which is guided by morphogens and cytogenesis and may provide guidance for the arealization of the brain.

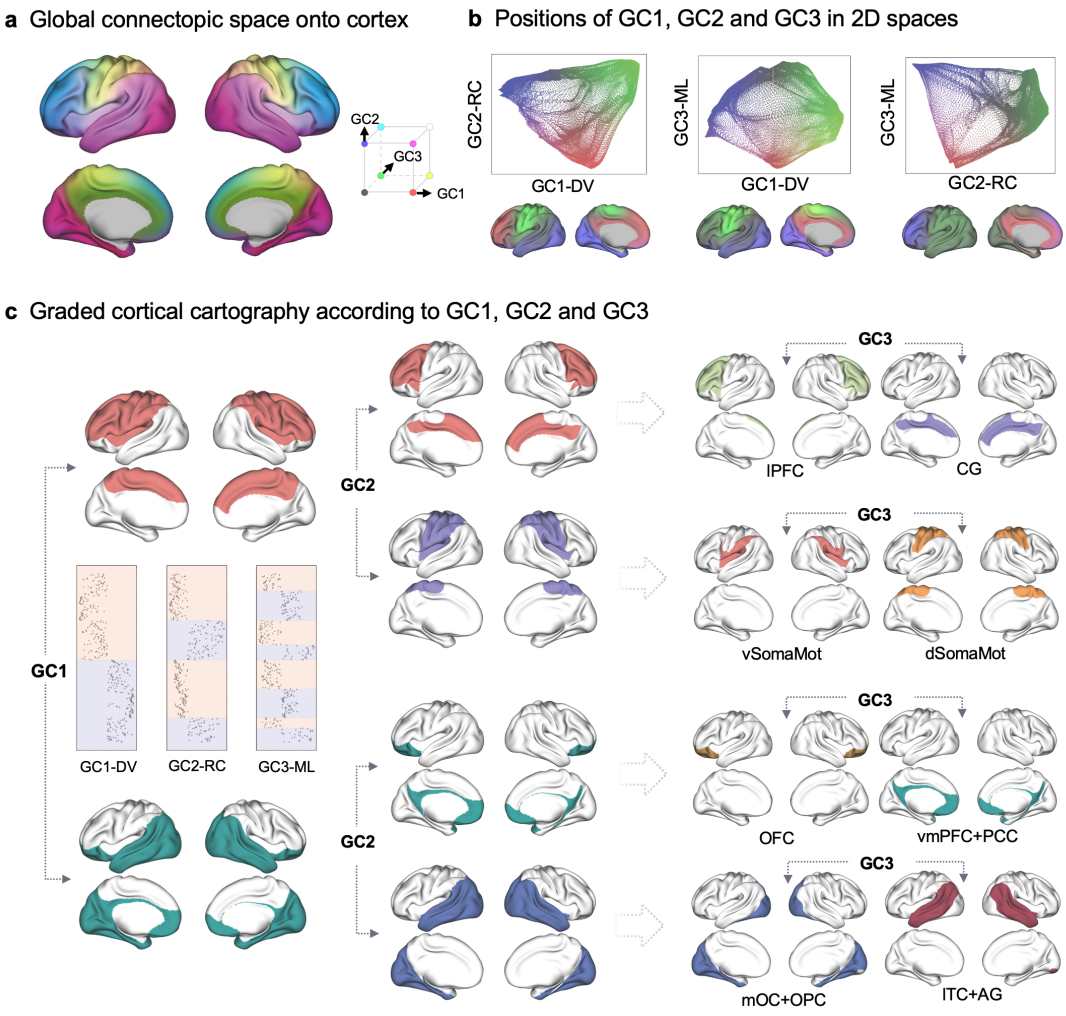

Figure 2. Global connectopies guide the process of arealization. (a) The three global connectopies were plotted together in what we termed the global connectopic space, with connectopy values assigned to the RGB values at each vertex. The global connectopic space integrates the information of three global connectopies and quantifies the topography of the dominant global connectopy. **(b)** Several lobes or subregions clearly appear when every two global connectopies are plotted together on the surface. GC1-DV and GC2-RC split the cortex into the prefrontal cortex and limbic cortex, sensorimotor and motor cortex, and occipitotemporal cortex. GC1-DV and GC3-ML split the cortex into the frontal cortex, limbic cortex, and occipitotemporal cortex. GC2-RC and GC3-ML split the cortex into the prefrontal cortex, limbic cortex, and other regions. **(c)** Partitioning of the brain by hierarchical clustering using the three global connectopies.

At each level, the brain was partitioned into two modules according to the positive and negative signs of the global connectopy. Eight modules, including lobes or functional networks, emerged clearly. vSomaMot ventral somatomotor cortex, dSomaMot dorsal somatomotor cortex, lPFC lateral prefrontal cortex, CG cingulate gyrus, lTC lateral temporal cortex, AG angular gyrus, mOC medial occipital cortex, OPC occipital polar cortex, OFC orbitofrontal cortex, vmPFC ventromedial prefrontal cortex, PCC posterior cingulate cortex.

Potential genetic basis underlying global connectopies

Having established the global connectopies in the human brain, we first explored the relationship between the genetic influence on cortical morphology with the identified global connectopies. We estimated the pairwise genetic correlation between vertices on the cortex using twin data from the HCP, which revealed shared genetic influences on cortical thickness and relative area expansion between cortical vertices. The first three gradients decomposed from the genetic correlation matrix of the surface area correspond with the three global connectopies (left: $r_{\text{GG1-Area, GC1-DV}} = 0.53$, $r_{\text{GG2-Area, GC2-RC}} = 0.49$, $r_{\text{GG3-Area, GC3-ML}} = 0.51$, all $p < .001$; right: $r_{\text{GG1-Area, GC1-DV}} = 0.58$, $r_{\text{GG2-Area, GC2-RC}} = 0.46$, $r_{\text{GG3-Area, GC3-ML}} = 0.51$, all $p < .001$). The first three gradients decomposed from the genetic correlation matrix of cortical thickness showed a rostral-caudal axis, a medial-lateral axis, and a dorsal-ventral axis (left: $r_{\text{GG1-Thickness, GC2-RC}} = 0.91$, $r_{\text{GG2-Thickness, GC3-ML}} = 0.72$, $r_{\text{GG3-Thickness, GC1-DV}} = 0.72$, all $p < .0001$; right: $r_{\text{GG1-Thickness, GC2-RC}} = 0.88$, $r_{\text{GG2-Thickness, GC3-ML}} = 0.71$, $r_{\text{GG3-Thickness, GC1-DV}} = 0.73$, all $p < .0001$; Figure 3a, 3b). Each parcel derived by the fuzzy clustering of the genetic correlation matrix of cortical thickness also showed significant overlap with one of the four parcels derived from the hierarchical clustering guided by the global connectopies (Figure 3c). These significant correspondence levels indicated a close genetic relatedness of the global connectopies.

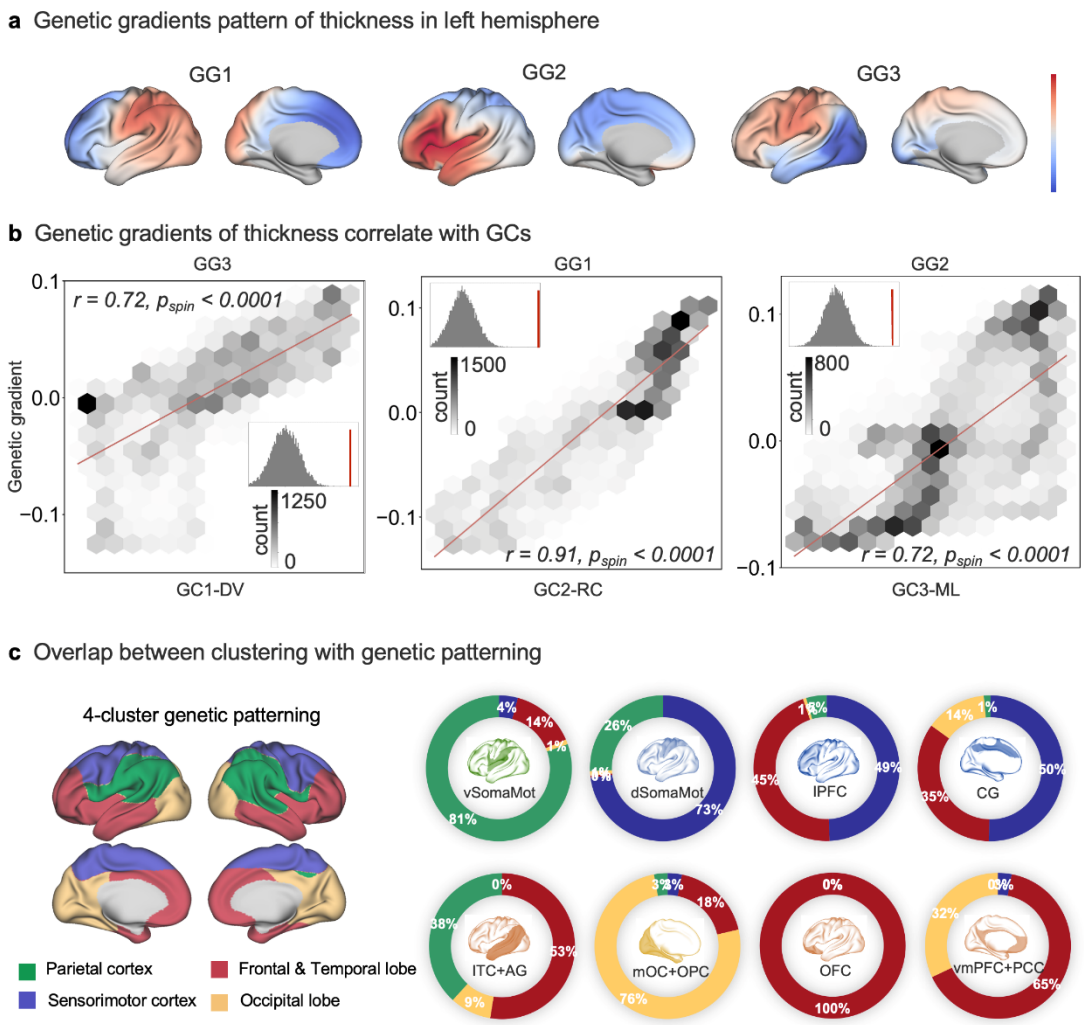

Figure 3. Global connectopies correspond to genetic topography. (a) The first three gradients of genetic similarity of cortical thickness. **(b)** The three gradients of genetic similarity of cortical thickness show a high correlation with global connectopies ($r_{\text{GC1-DV, GG3-Thickness}}$=0.72, $r_{\text{GC2-RC, GG1-Thickness}}$=0.91, $r_{\text{GC3-ML, GG2-Thickness}}$=0.72, all p<0.0001). **(c)** Overlap between four modules derived from hierarchical clustering with genetic patterning of cortical thickness.

We next explored the roles of the genes that contributed to the global connectopies. Here we focused on the genes in the top 5% of each global connectopy (corrected for multiple comparisons). We found that a selection of genes contributed to more than one global connectopy, with 22 genes overlapping with all three (Figure 4a right). Gene enrichment analyses using different gene sets showed that genes that contributed to only one global connectopy, especially GC2-RC, were involved with biological processes (Figure 4c). The top genes in each global connectopy, such as *FARSA*, *MPND*, *SYCP2*, *CUX1*, *ARHGDIG*, and *NUDT14*, are known to be associated with the

regulation of transcription factor activity, morphogenesis, cell proliferation, and metabolic processes (Figure 4b) [57-63]. Genes related to all three global connectopies showed an obvious connection with various diseases (Figure 4c), with the top genes including *ADAMTSL1* and *TIAM1*, whose mutations can cause several diseases (Figure 4b) [64-66]. Digging deeper into specific biological processes, we found an enrichment of terms related to the regulation of transcription, metabolic process, morphogenesis, cellular development, and neuron projection (Figure 4d).

Exploring the developmental pattern of the genes associated with global connectopies, we found that these genes were expressed highly in the prenatal period in all lobes and that their expression decreased after birth (Figure 4e), suggesting that the patterns present in adulthood were nearly reached in the early stages of development.

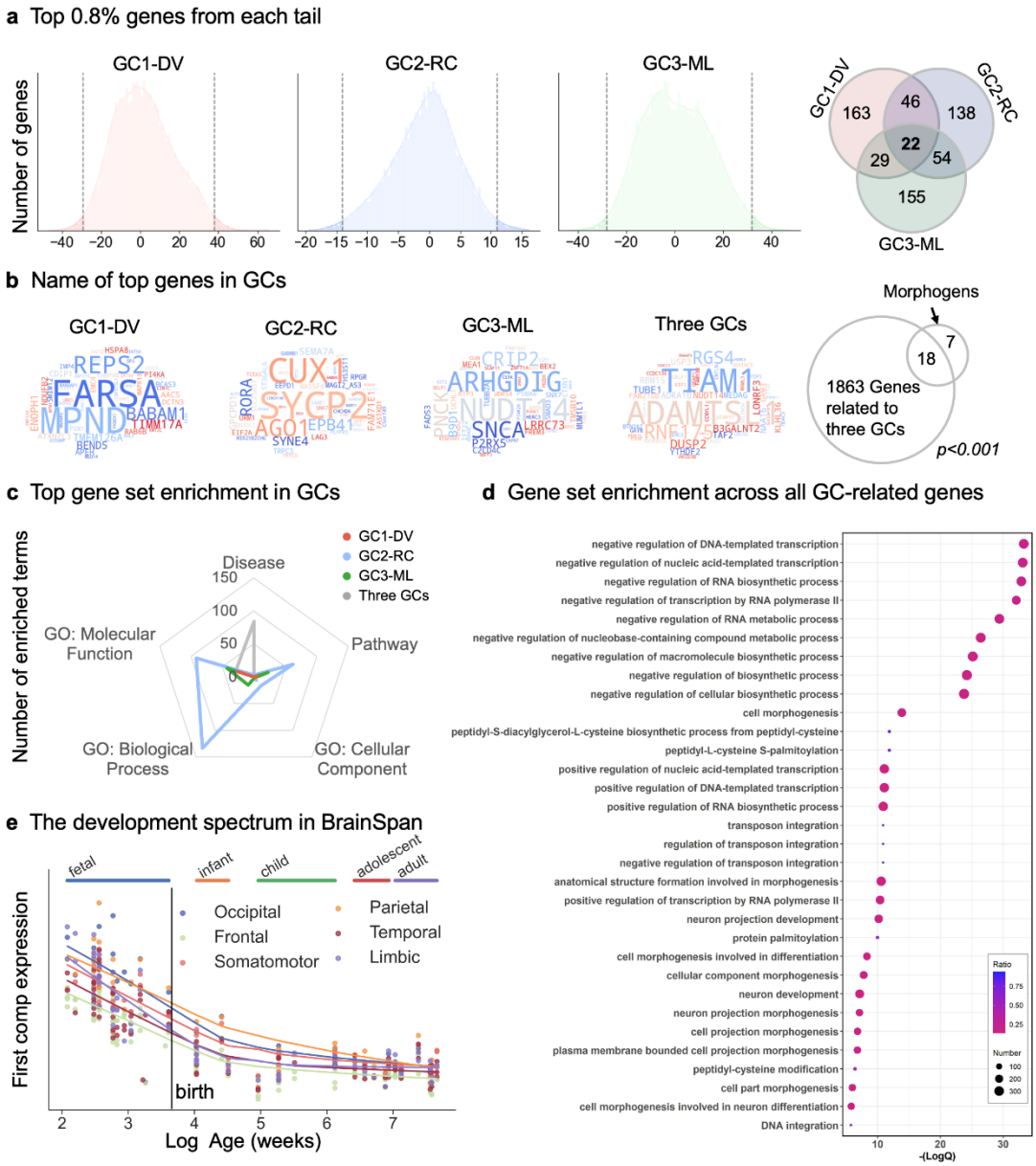

Figure 4. Gene enrichment analysis of connectopy-associated genes. (a) Distributions of connectopic weights across genes. Genes in the top 0.8% of either tail of the distribution (n = 130) were selected for further enrichment analysis. The Venn diagram showing the overlap of genes is shown on the right. **(b)** Top genes for unique connectopy and overlap of connectopies. **(c)** Gene set enrichment was conducted on genes belonging to each global connectopy and all three connectopies. **(d)** Gene set enrichment across all global connectopy-related genes indicated terms related to the regulation of transcription, metabolic process, morphogenesis, cellular development, and neuron projection. **(e)** The development spectrum of gene expression for each brain macrostructure. Genes associated with global connectopies were expressed highly in the prenatal period and decreased after birth.

Since the morphogen gradients have been established and their pattern was conserved during the development [22], we explored whether these genetic patterns correspond with those of the structural connectivity. We first identified the genes in AHBA that are strongly expressed in one end of the brain, according to a previous publication [54]. 18 of these genes overlapped with the genes identified to contribute to three global connectopies (hypergeometric test, p<0.001; Figure 4B). Then we subdivided the connectopies equally into eight parts. Paired t-tests was used to assess the difference of gene expression of these genes between the first and the last cluster. We found expression of *FGF17* was significantly higher in the dorsal cluster than the ventral cluster (t=27, p<.001), while expression of *FOXG1* was significantly higher in the ventral (t=-25, p<.001). The same opposite patterns were observed between *BMP7* (rostral<caudal, t=-33, p<.001) and *PAX6* (rostral>caudal, t=29, p<.001), and *SFRP1* (medial<lateral, t=-41, p<.001) and *WNT3* (medial>lateral, t=99, p<.001) (Figure 5a). The number of subdivisions do not affect the final results (Figure S16).

We also showed that the three global connectopies showed significant correlations with the spatiomolecular gradients found in [22] ($r_{GC1\text{-}DV, LV1}$ = 0.74, p < .001; $r_{GC2\text{-}RC, LV2}$ = 0.75, p < .001; $r_{GC3\text{-}ML, LV3}$ = 0.5, p = .002) (Figure 5b). Note that the gradient values for the subcortex, cerebellum, and brainstem were excluded, and only data for the cortex were considered. Since the LV3 gradient showed the most variation and varied along a mediolateral and dorsoventral direction, as mentioned in [22], the r-value was lower compared with the former two but still significant, and the correlation between the first global connectopy was also moderate ($r_{GC1\text{-}DV, LV3}$ = -0.36, p < .05). These again

suggested a potential genetic basis underlying the global connectopies.

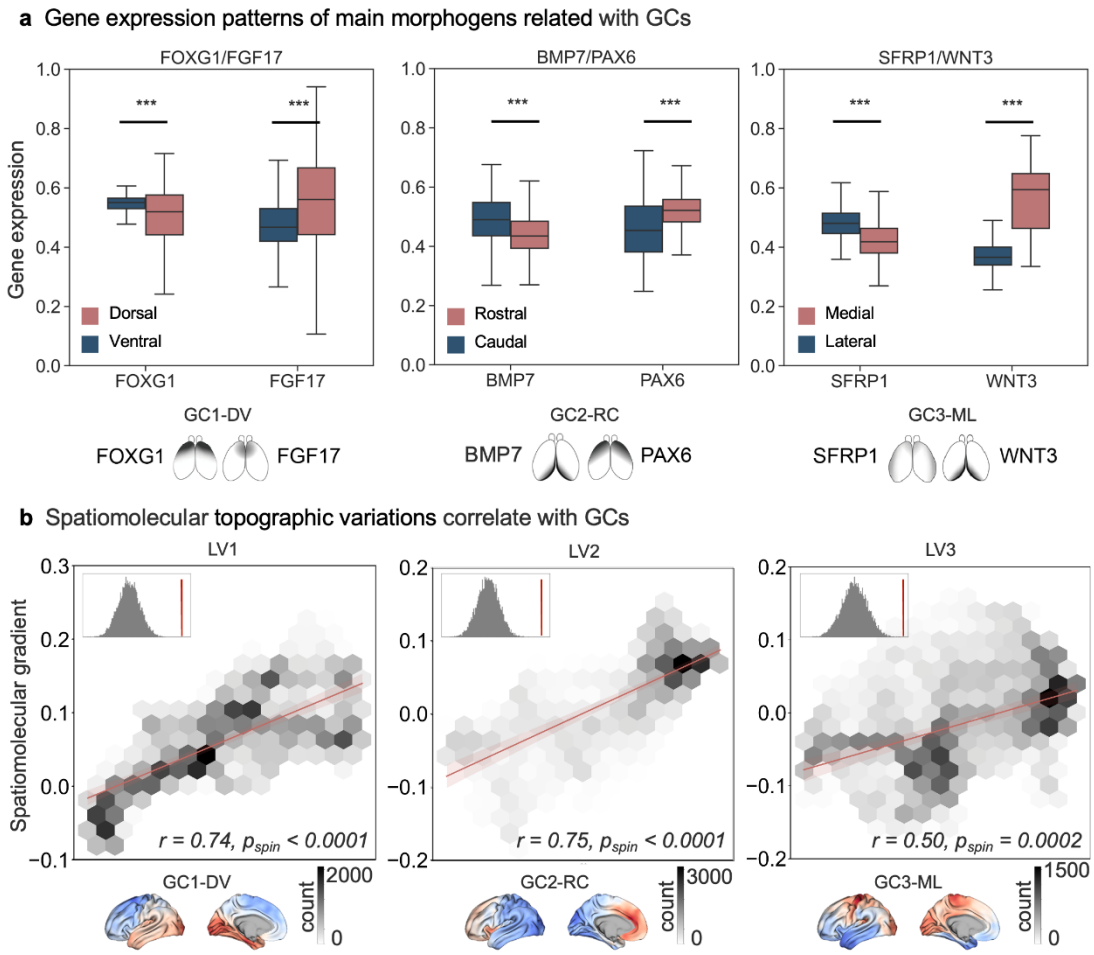

Figure 5. Potential genetic basis underlying global connectopies. (a) The expression of genes was significantly different between the two ends of the global connectopies (paired t-test, all p<.001). **(b)** The global connectopies significantly correlated with the spatiomolecular gradients ($r_{\text{GC1-DV, LV1}}$ = 0.74, p < .001; $r_{\text{GC2-RC, LV2}}$ = 0.75, p < .001; $r_{\text{GC3-ML, LV3}}$ = 0.5, p = .002).

The three connectopies are situated by distinct sets of white matter tracts

Since genes and morphogens govern the process of morphogenesis, establishing the positions of specific cells as well as the formation of neuronal projections, i.e., axons, whose courses are believed to guide cortical differentiation, we finally explored how the underlying white matter shaped these spatial organizations. We first projected the global connectopic space onto the white matter. Specifically, every white matter voxel was assigned to the connectopy value of the vertex to which it had the strongest connection strength (Figure 6a). For each white matter voxel, the value of the

vertex that had the strongest connection strength was extracted to produce a voxel projection map. We similarly generated a projection map for each global connectopy (Figure 6b).

As expected, the results showed the same pattern as that for the gray matter (Figure 3b). For GC1-DV, the white matter voxels were distributed along the ventral-dorsal axis beneath the surface. Specifically, voxels lying near the sensorimotor/motor cortex and occipitotemporal cortex showed values that were markedly consistent with the locations of the extremes of the first global connectopy. Voxels corresponding to GC2-RC and GC3-ML varied from posterior to anterior and medial to lateral.

To verify our results, we also fitted general linear models (GLMs) to measure the relationship between white and gray matter. The results revealed that white matter voxels near the brain regions that anchored the extremes of global connectopies had high values, consistent with the above findings (Figure S18).

Since the white matter is mainly composed of tracts, we then focused on the specific tracts related to the emergence of the global connectopies. We reconstructed 72 fiber bundles following TractSeg [38] (Table S1) and built group-level connectivity fingerprints. Figure S4c shows the distribution of the fingerprint along the global connectopies. We also generated global connectopies based on the connectivity fingerprint following the same procedure (Figure S4a). Specifically, we built a TC matrix by correlating pairs of vertices from the connectivity fingerprint and also used diffusion map embedding. The global connectopies generated by the fingerprints were very similar to the results calculated by the original structural connection (Figure 1b, Figure S4a; Left: $r_{\text{GC1-DV}} = 0.91$, $r_{\text{GC2-RC}} = 0.86$, $r_{\text{GC3-ML}} = 0.65$; Right: $r_{\text{GC1-DV}} = 0.94$, $r_{\text{GC2-RC}} = 0.82$, $r_{\text{GC3-ML}} = 0.53$), indicating that low-dimensional connectivity fingerprints captured most of the structural connectivity information in the brain.

We then produced tract projection maps by masking out voxels not situated on the tract. By calculating the mean value and variance of the voxels in each tract (Figure 3c), we identified the tracts that were either situated at one of the extremes of the global connectopy or were spread out along the axis. The results for the bilateral tracts were averaged between the two hemispheres and are shown in the scatterplot.

Two types of characteristic tracts are shown in the right columns of Figure 6c, including T_PREC, ST_OCC, and T_PAR for GC1-DV as well as MLF, T_PREF, SLF_II for GC2-RC along

with AF, CG, and ST_PAR for GC3-ML (The voxel-level contributions of all tracts are shown in Figure S20-22).

For GC1-DV, the thalamo-precentral tract (T_PREC), which connects the thalamus with the precentral gyrus, is related to motor task performance [67,68]. T_PREC has a distinctly vertical expanding shape and showed high mean values near the dorsal end of GC1-DV, thus expressing the most significant contribution to the global connectopy. The striato-occipital (ST_OCC) tract connects the striatum with the occipital cortex, showing high mean values at the ventral end and having a "stretching" impact on the global connectopy pattern. In contrast, the thalamo-parietal tract (T_PAR) has a high variance within the GC1-DV and appears to constrain the global connectopy formation.

For GC2-FC, the second branch of the superior longitudinal fascicle (SLF_II), which mostly runs from the posterior to the anterior, starting from the middle frontal gyrus and terminating in the angular gyrus, had the greatest mean value for the white matter tract. The SLF_II, which covered most of the areas in the second global connectopy, also showed high values, providing the prefrontal cortex with parietal cortex information about the perception of visual space and providing information about working memory in the prefrontal cortex to the parietal cortex to focus spatial attention and regulate the selection of spatial information [69,70]. Other "high-contribution" tracts, including the MLF and T_PREF, are either in the anterior or posterior regions.

The GC3-ML showed a similar pattern to the tracts that made high contributions. The corpus callosum, the giant white matter fiber bundle consisting of millions of axonal projections, spans from the medial brain through the different parts of the cortex and connects all the brain lobes. Thalamo- and striato-cortical projections also project from the subcortical nuclei and reach the different lateral cortices. We suggest that the former type of tract plays a role in stretching the brain along the axis while the latter type has a constraining effect and that these two work together to shape the organization of the brain.

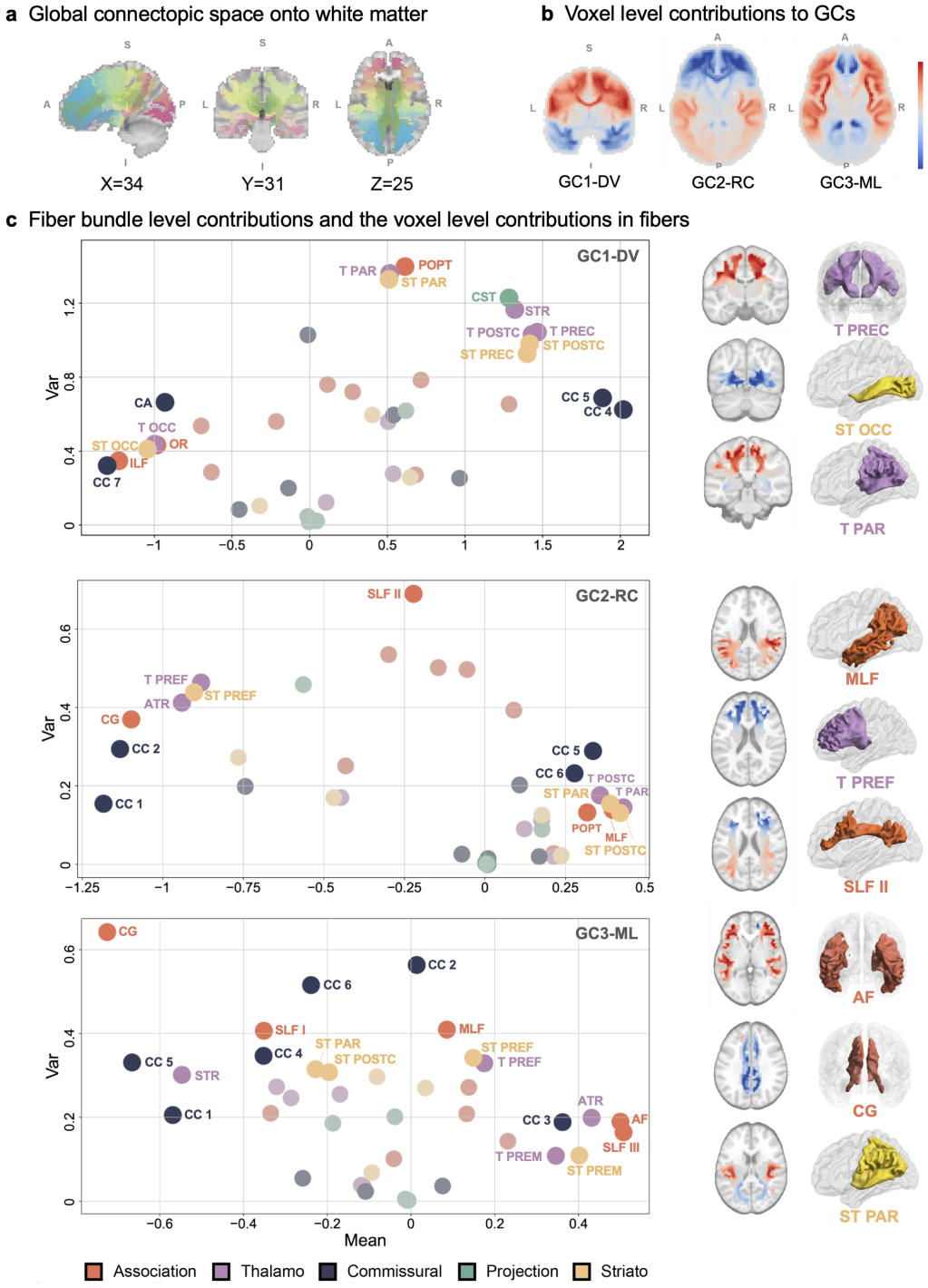

Figure 6. The three global connectopies are situated by distinct sets of white matter tracts. (a) Projection of the global connectopic space onto the white matter. **(b)** Projection of the global connectopies onto the white matter, showing the voxel contribution to the global connectopies. The results for the white matter were consistent with those for the gray matter. **(c)** Mean values and variances of the contribution of five types of tracts to the global connectopies. Each dot represents one tract. Different colors represented different types of tracts, with deeper colors for higher

contributions. The right two columns show two types of characteristic tracts contributing to the global connectopies, with one type of tract situated at one extreme of the global connectopy and the other stretched across the global connectopy. The first column shows the voxel-level contributions to the tract, and the second shows the corresponding fiber bundles reconstructed by TractSeg.

Discussion

In the current study, we demonstrated that a low-dimensional, topological representation of brain connectivity exists and may share common space with gene expression, linking the accurate formation of connections and cortical arealization despite the significant disparity in the numbers of genes and connections. We systematically analyzed the spatial topography of cerebral connectivity, i.e., the white matter tractogram, and identified three orthogonal global connectopies: the dorsoventral, rostrocaudal, and mediolateral connectopy across the cerebral cortex. Moreover, the global connectopies were observed to be aligned with the gradients of morphogens identified during embryonic brain development and with genetic topography and spatiomolecular gradients. Our findings suggest that the observed global connectopies may link genetic drivers with the formation of cortical patterns and that they are represented in the spatial arrangement of long-range white matter tracts. Together, our findings demonstrate the crucial role that comprehending the connectivity topographies and their genetic constraint plays in understanding the underlying principles that shape the human brain organization.

Linking cortical patterning and genetic gradients through the global connectopies

Our findings showed that the three global connectopies derived from the white matter characterized the embedding of connectivity architecture underlying the cortex in a low dimensional space organized along the dorsoventral, rostrocaudal, and mediolateral axes, which closely resemble the principal axes of brain development [22,71] and the chemotactic gradients of early embryogenesis [72,73]. From a developmental perspective, both the encoding of chemical gradients by morphogenes and the spatial expression patterns of all genes during the formation of the mature brain, along with recent research on phenotypic mapping facilitated by twin studies [1-3], indicate that gradient-based organizational principles may serve as one of the fundamental rules in the precise formation of gene-encoded connections and the establishment of functional cortical regions. Meanwhile, genes provide the initial blueprint that guides differentiation and the directional migration of neurons through the subsequent formation of different types of gradients of transcription factors, morphogenes, etc., and, in parallel, the precise trajectory and projection of axons [74]. However, the reality is likely somewhere in between that a few dozen molecules (rather than a few or a thousand) enact pattern formation rules to increase the probability that neurons make the correct connections. Despite their daunting

complexity, these wiring pattern formations are likely governed by simple rules. The scaffolding rule guides the exact formation of neural circuit [75], wherein genes might not drive the precise details of complex circuit diagrams but have the potential to influence their organizational rules during development [25]. Here, the observed global connectopies could be one of the possible rules, which are logically consistent with the argument that integrating different types of gradients guides and drives cortical patterning during early brain development [76]. Therefore, by reconsidering the underlying driving forces behind the formation of the cortical organization, we highlighted the irreplaceable role of anatomical connection, which may bridge the gap from transcriptional expression to cortical arealization in the brain.

The dorsoventral and rostrocaudal genetic topographies (Figure 3) observed in our study suggest genetic influences on cortical morphology where regional differentiation is controlled by genes expressing a graded pattern [1,2,77,78]. More interestingly, we not only observed a high correspondence between gene topology and our global connectopies but also performed a hierarchical cortical parcellation and found that the results resemble closely with the parcellation obtained using genetic correlation [2]. This correspondence indicates the presence of the same graded pattern across the cortex at the genetic and connectional levels and is also consistent with the gradation of architectonic features. The connectivity between cortical layers is related to their architectonic features and may provide evidence for the role of connections in the initial scaffolding for cortical organization. In other words, cortical patterning and genetic topography may link through the global connectopies. Previous research found that cortical patterning creates segregated areas with different functions via cell differentiation and migration. These segregated areas specifically occur along molecular gradients representing the patterned expression of morphogens and transcription factors [17,76]. We found that the genes related to the identified global connectopies coded for known morphogens and transcription factors (Figure 4). These factors were especially involved in biological processes, including regulation of transcription, metabolic process, morphogenesis, cellular development, and neuron projection. In addition, the genes associated with all the global connectopies were found to be more related to brain diseases. This finding is consistent with the observation that disruptions in forming early developmental gradients through mutations to gradient-associated genes can cause severe developmental disorders [22,79]. These associations demonstrated that global connectopies and their underlying genetic basis were essential to the

development and function of the brain.

The morphogen gradients of the developing brain were previously established and found to radiate along the rostrocaudal, dorsoventral, and mediolateral axes of the neural compartment [80]. These are conserved to maturity [22] and are consistent with our global connectopies (Figure 5A). At maturity, the morphogen gradients are replaced by a more distinct and discrete regional gene expression [54]. Under the effect of morphogens secreted in the patterning centers with absolute positional information, numerous transcription factors are expressed in a graded manner. For example, the anterior expression of *FGF8* suppresses the posteriorly expressed transcription factors, resulting in their lower anterior but higher posterior expression [81]. *FGF8* was also reported to stimulate the proliferation of cortical progenitor cells, thus regulating neurogenesis and arealization by thalamic axons [82]. Similarly, manipulation of the transcription factor *EMX2* by genetic knockout resulted in finding higher expression posteromedially, as well as finding that a lower expression anterolaterally causes an expansion of the frontal and lateral regions at the expense of the visual cortex in mice [83]. These transcription factors are believed to determine the areal fate and the expression of cell-surface molecules, thus determining the topographic organization of synaptic inputs and outputs [1,23] and directing axonal outgrowth [24].

Many existing studies of thalamocortical and corticothalamic projections have identified specific receptors and ligands, such as the Eph receptor tyrosine kinases and their ephrin ligands, that are required to establish proper patterns of afferent and efferent cortical connectivity with subcortical structures [84,85]. However, whether these molecules play a similar role in instructing intracortical connectivity within the developing cortex is unclear. Relevant studies in this regard, such as in utero electroporation studies [86] and a study during primate development [87], suggest that directed axonal growth and target selection play a role in forming association projections between specific cortical areas. Moreover, according to the radial unit hypothesis of cortical development, radial glial cells in the embryonic brain facilitate the generation, placement, and allocation of neurons in the cortex and regulate how they wire up [88,89]. The radial glial scaffold might act as a "highway" for axons, facilitating their growth and ensuring their proper trajectories. Nevertheless, the factors that drive the competence of specific axons to grow into select gray matter regions are unknown, but molecular interactions between axons and recipient cortical areas may be involved [74]. Here, our current findings only identified associations between gene gradients and global

connectopies in adult brains. Although we also did an integrated lifespan analysis of genes that appear to contribute to the connectopies, providing possible correlations, further studies are needed to explain the dynamics and causality during early development directly. In future studies, the progress of new technologies [90,91] should be particularly helpful here and hopefully enable a clearer explanation of these relationships.

The global connectopies orchestrate flexible functions across the cortex

As the anatomical backbone of macroscale functional hierarchy, invariant white matter can scaffold many flexible cognitive processes. We demonstrated in this study that the dorsoventral, rostrocaudal, and mediolateral axes could provide new insights into the emergence of functions within this connected architecture.

The first, the dorsoventral global connectopy (GC1-DV), explained the greatest amount of variance. It had a similar topography to the second functional gradient [28], with the visual and sensorimotor cortex anchored at the two ends of the global connectopy. This was confirmed by the result of NeuroSynth decoding, i.e., the ventral and dorsal parts of the cortex were proposed to have different cognitive functions, with the dorsal part related to “foot” or “finger” and the ventral part linked to “navigation” or “episodic”, which corresponds to the distribution of the global connectopy on the intrinsic functional network. First, following the dual origin theory that the cerebral cortex evolved from two primordial brain structures and finally formed functionally distinct ventral and dorsal systems [92,93], we identified the first principal component of the structural connection along the same axis. Pandya and others demonstrated that cortico-cortical connections are ordered consistently with the dorsoventral division and that long cortico-cortical tracts provide reciprocal pathways [94-97]. More interestingly, the GC1-DV was related to the principal functional gradient found in neonates [98] and children (under 12 years old), which shifts to a pattern that transitions from the unimodal to the association cortex during development [99]. Since synaptogenesis and pruning in the unimodal cortex occur earlier, the association cortex goes through a protracted period of synaptic development with the formation of experience, memory, and semantics at a mature age [100,101] when the unimodal-association gradient emerges and becomes the principal functional gradient. This indicates that a stable structural connection might be the foundation of the functional organization of the cortex. Moreover, GC1-DV, varying along the sensory–association–motor axis, might be the

place where the basic input-central processing-output information processing occurs. This change could be explained by changes in the dimensionality of multitask representations across this hierarchy, which are first compressed from the sensory to the association areas and then expanded from the association to the motor areas (Figure S3) [102]. When we explored the white matter tracts that may contribute to the GC1-DV, we found that projection tracts, such as the thalamo-precentral tract and striato-occipital tract, contribute the most to the formation of the dorsoventral pattern. Because they are the sources of all external sensory information, the thalamocortical projections appeared in the earliest organisms, followed by the corpus callosum and association tracts in the mammalian brain [103-106].

For the second rostrocaudal global connectopy (GC2-RC), previous studies have provided converging evidence for the existence of the anterior-posterior axis. For example, neuron density decreases, and neuronal connectivity increases from the posterior to the anterior brain areas. This can be attributed to differences in neurogenesis between the posterior and anterior areas [27]. These graded cytoarchitectural patterns reflect the local structural connection. When we studied the oscillational features of the brain, GC2-RC showed a remarkable relationship with several bands of MEG maps and had the same pattern as the spatial gradient of the dominant peak frequency of the oscillations [107]. Since the cerebral cortex shows characteristic spectral activity patterns, with alpha activity strongest in occipitoparietal areas, beta activity strongest in sensorimotor areas, and delta and theta activity strongest in prefrontal brain areas [108-110], we suggest that global connectopies, as the anatomical structure, might shape the rhythmic neuronal activity of the brain, thus playing a central role in coordinating neuronal activity.

The third global connectopy, i.e., GC3-ML, which varied from the medial to the lateral areas, showed the most variation and, of the three global connectopies, had the highest correlation with inter-subject variance in functional connectivity [111]. Considering the distance map from archicortical and paleocortical formations, the vertices on the cerebral cortex showed a distance from the two primordial brain structures along a medial-lateral axis, corresponding to the mediolateral axis during development. As to the tracts with high contributions of GC3-ML, except for the corpus callosum, the thalamo- and striato-cortical projections also project from the subcortical nuclei and reach different lateral cortices. Recent studies demonstrated that thalamic axons are routed to different cortical areas before entering the cortex by the organized interareal topography of thalamocortical

projections in the ventral forebrain [104,112,113]. These give evidence that topographically organized structural connections shape the process of development of the cerebral cortex into distinct cortical areas underlying different cognitive functions.

Methodological consideration and future work

Several technical and methodological limitations must be acknowledged in the current work. The first and most direct concern is the accuracy of mapping structural connections using diffusion tensor imaging. However, diffusion tractography has been used as an irreplaceable tool to identify white matter across the brain *in vivo* and non-invasively, with certain limitations imposed by the tractography, such as gyral bias, which can cause false positive results [114,115]. In the future, joint MRI and microscopy data analysis may help solve limitations [116-118]. Alternatively, cutting-edge invasive neuro-techniques used in other mammalian cortexes, such as Cre-drivers for cortical projection mapping [119] or polarised light imaging [120,121], could be used at the mesoscale level of resolution to study whether such organizational axes are conserved across scales and species. Distance effect also needs to be considered when mapping the structural connectivity pattern, but the consistent genetic topography of the three global connectopies suggests that they are not distance-dependent. Interestingly, a recent study challenged traditional views and showed that the geometry of the brain had a more fundamental role in shaping its function than interregional connectivity [122]. Although the association between cortical geometry and brain function should be recognized, the causal relationship between them can only be revealed by considering genes, which are the most essential and determining. Secondly, the parcellation guided by the three global connectopies is very coarse compared with several fine-grained brain atlases that have been delineated using the gradient approach [33,123]. We did not utilize these more fine-grained parcels because we believe they are more likely to be shaped by local gradients compared with the three global connectopies, which characterize the global pattern across the brain.

In this study, we mainly focused on the structural connectivity patterns shown on the cortex and brought functional emergence into the discussion. More thorough microscale biological foundations and physiological processes were not explored here, but in future studies, they may aid in interpreting our findings about macroscale structural patterns. Since the spatiomolecular gradients expressed in childhood and adulthood have been established and shown to be consistent [22], an

immediate goal will be to explore the transition in structural patterns throughout development. Whether these global connectopies are conserved across species could be another perspective to study when looking into the organization of the brain. We also need animal studies to validate or study the causal relationships between the genes, connectivity, and parcellations. In addition, the observed organizing principles in the current work may also be used to guide the engineering of three-dimensional cortical spheroids and to comprehend the human-specific aspects of the neural circuit assembly [124,125].

Conclusions

To conclude, we explored how genes link the accurate formation of connections, despite significant differences in their numbers and how they constrain cortical arealization. Our research uncovered three determinant spatial trends across the cerebral cortex, aligning with the dorsoventral, rostrocaudal, and mediolateral axes, which we identified as global connectopies. These global connectopies were found to align with spatiomolecular gradients and might scaffold the cortical patterning. Our findings revealed the existence of a low-dimensional, topological representation of brain connectivity that may share a common space with gene expression, scaffolding the proper formation of connections and cortical arealization. We hope our discoveries will offer valuable insights into studying brain structure and function.

Data availability

Data from Human Connectome Project can be downloaded at https://db.humanconnectome.org/. The activated maps of cognitive terms can be downloaded from the NeuroSynth database (https://neurosynth.org/). The human gene expression data are available in the Allen Brain Atlas (https://human.brain-map.org/static/download). Data from BrainSpan can be downloaded at https://www.brainspan.org/.

Code availability

The HCP-Pipeline can be found at https://github.com/WashingtonUniversity/HCPpipelines. The neuroimaging preprocessing software used for the other datasets is freely available (FreeSurfer v6.0, http://surfer.nmr.mgh.harvard.edu/, and FSL v6.0.5, https://fsl.fmrib.ox.ac.uk/fsl/fslwiki). The gene processing pipeline is available (abagen, https://github.com/rmarkello/abagen), and gene enrichment analysis is conducted at https://toppgene.cchmc.org/. The brain maps were presented using BrainSpace (https://brainspace.readthedocs.io/) and Workbench v1.5.0 (https://www.humanconnectome.org/software/connectome-workbench). The tracts were visualized using BrainNet Viewer v1.7 (https://www.nitrc.org/projects/bnv/).

Acknowledgments

This work was partially supported by STI2030-Major Projects (Grant No. 2021ZD0200200), the Natural Science Foundation of China (Grant Nos. 82072099, 82202253, 62250058), and the Strategic Priority Research Program of the Chinese Academy of Sciences (XDB32030200), and the China Postdoctoral Science Foundation (2022M722915). Data were provided in part by the Human Connectome Project, WU-Minn Consortium (Principal Investigators: David Van Essen and Kamil Ugurbil; 1U54MH091657) funded by the 16 NIH Institutes and Centers that support the NIH Blueprint for Neuroscience Research; and by the McDonnell Center for Systems Neuroscience at Washington University. The authors appreciate the English language and editing assistance of Rhoda E. and Edmund F. Perozzi, PhDs.

Declaration of interests

The authors declare no competing interests.

References

1 Chen, C. H. *et al.* Genetic topography of brain morphology. *Proc Natl Acad Sci U S A* **110**, 17089-17094, doi:10.1073/pnas.1308091110 (2013).

2 Chen, C. H. *et al.* Hierarchical genetic organization of human cortical surface area. *Science* **335**, 1634-1636, doi:10.1126/science.1215330 (2012).

3 Chen, C. H. *et al.* Genetic influences on cortical regionalization in the human brain. *Neuron* **72**, 537-544, doi:10.1016/j.neuron.2011.08.021 (2011).

4 Huang, Y. *et al.* Mapping Genetic Topography of Cortical Thickness and Surface Area in Neonatal Brains. *J Neurosci*, doi:10.1523/JNEUROSCI.1841-22.2023 (2023).

5 Zhao, B. *et al.* Heart-brain connections: Phenotypic and genetic insights from magnetic resonance images. *Science* **380**, abn6598, doi:10.1126/science.abn6598 (2023).

6 Burt, J. B. *et al.* Hierarchy of transcriptomic specialization across human cortex captured by structural neuroimaging topography. *Nat Neurosci* **21**, 1251-1259, doi:10.1038/s41593-018-0195-0 (2018).

7 Greig, L. C., Woodworth, M. B., Galazo, M. J., Padmanabhan, H. & Macklis, J. D. Molecular logic of neocortical projection neuron specification, development and diversity. *Nat Rev Neurosci* **14**, 755-769, doi:10.1038/nrn3586 (2013).

8 Molnar, Z. *et al.* New insights into the development of the human cerebral cortex. *J Anat* **235**, 432-451, doi:10.1111/joa.13055 (2019).

9 Srinivasan, K. *et al.* A network of genetic repression and derepression specifies projection fates in the developing neocortex. *Proc Natl Acad Sci U S A* **109**, 19071-19078, doi:10.1073/pnas.1216793109 (2012).

10 Fan, L. *et al.* The Human Brainnetome Atlas: A New Brain Atlas Based on Connectional Architecture. *Cereb Cortex* **26**, 3508-3526, doi:10.1093/cercor/bhw157 (2016).

11 Passingham, R. E., Stephan, K. E. & Kotter, R. The anatomical basis of functional localization in the cortex. *Nat Rev Neurosci* **3**, 606-616, doi:10.1038/nrn893 (2002).

12 Braun, U. *et al.* Dynamic reconfiguration of frontal brain networks during executive cognition in humans. *Proc Natl Acad Sci U S A* **112**, 11678-11683, doi:10.1073/pnas.1422487112 (2015).

13 Cui, Z. *et al.* Optimization of energy state transition trajectory supports the development of executive function during youth. *Elife* **9**, doi:10.7554/eLife.53060 (2020).

14 Gu, S. *et al.* Controllability of structural brain networks. *Nat Commun* **6**, 8414, doi:10.1038/ncomms9414 (2015).

15 Talozzi, L. *et al.* Latent disconnectome prediction of long-term cognitive-behavioural symptoms in stroke. *Brain* **146**, 1963-1978, doi:10.1093/brain/awad013 (2023).

16 Thiebaut de Schotten, M., Foulon, C. & Nachev, P. Brain disconnections link structural connectivity with function and behaviour. *Nat Commun* **11**, 5094, doi:10.1038/s41467-020-18920-9 (2020).

17 Cadwell, C. R., Bhaduri, A., Mostajo-Radji, M. A., Keefe, M. G. & Nowakowski, T. J. Development and Arealization of the Cerebral Cortex. *Neuron* **103**, 980-1004, doi:10.1016/j.neuron.2019.07.009 (2019).

18 Dickson, B. J. Molecular mechanisms of axon guidance. *Science* **298**, 1959-1964, doi:10.1126/science.1072165 (2002).

19 Price, D. J. *et al.* The development of cortical connections. *Eur J Neurosci* **23**, 910-920, doi:10.1111/j.1460-9568.2006.04620.x (2006).

20 Stoeckli, E. T. Understanding axon guidance: are we nearly there yet? *Development* **145**, doi:10.1242/dev.151415 (2018).

21 Hawrylycz, M. *et al.* Canonical genetic signatures of the adult human brain. *Nat Neurosci* **18**, 1832-1844, doi:10.1038/nn.4171 (2015).

22 Vogel, J. W. *et al.* Conserved whole-brain spatiomolecular gradients shape adult brain functional organization. *bioRxiv* (2022).

23 Rubenstein, J. L. & Rakic, P. Genetic control of cortical development. *Cereb Cortex* **9**, 521-523, doi:10.1093/cercor/9.6.521 (1999).

24 Chilton, J. K. Molecular mechanisms of axon guidance. *Dev Biol* **292**, 13-24,

doi:10.1016/j.ydbio.2005.12.048 (2006).

25 Hassan, B. A. & Hiesinger, P. R. Beyond Molecular Codes: Simple Rules to Wire Complex Brains. *Cell* **163**, 285-291, doi:10.1016/j.cell.2015.09.031 (2015).

26 Shen, E. H., Overly, C. C. & Jones, A. R. The Allen Human Brain Atlas: comprehensive gene expression mapping of the human brain. *Trends Neurosci* **35**, 711-714, doi:10.1016/j.tins.2012.09.005 (2012).

27 Huntenburg, J. M., Bazin, P. L. & Margulies, D. S. Large-Scale Gradients in Human Cortical Organization. *Trends Cogn Sci* **22**, 21-31, doi:10.1016/j.tics.2017.11.002 (2018).

28 Margulies, D. S. *et al.* Situating the default-mode network along a principal gradient of macroscale cortical organization. *Proc Natl Acad Sci U S A* **113**, 12574-12579, doi:10.1073/pnas.1608282113 (2016).

29 Van Essen, D. C. *et al.* The WU-Minn Human Connectome Project: an overview. *Neuroimage* **80**, 62-79, doi:10.1016/j.neuroimage.2013.05.041 (2013).

30 Glasser, M. F. *et al.* The minimal preprocessing pipelines for the Human Connectome Project. *Neuroimage* **80**, 105-124, doi:10.1016/j.neuroimage.2013.04.127 (2013).

31 Robinson, E. C. *et al.* MSM: a new flexible framework for Multi-modal Surface Matching. *Neuroimage* **100**, 414-426, doi:10.1016/j.neuroimage.2014.05.069 (2014).

32 Vertes, P. E. *et al.* Gene transcription profiles associated with inter-modular hubs and connection distance in human functional magnetic resonance imaging networks. *Philos Trans R Soc Lond B Biol Sci* **371**, doi:10.1098/rstb.2015.0362 (2016).

33 Schaefer, A. *et al.* Local-Global Parcellation of the Human Cerebral Cortex from Intrinsic Functional Connectivity MRI. *Cereb Cortex* **28**, 3095-3114, doi:10.1093/cercor/bhx179 (2018).

34 Glasser, M. F. *et al.* A multi-modal parcellation of human cerebral cortex. *Nature* **536**, 171-178, doi:10.1038/nature18933 (2016).

35 Behrens, T. E., Berg, H. J., Jbabdi, S., Rushworth, M. F. & Woolrich, M. W. Probabilistic diffusion tractography with multiple fibre orientations: What can we gain? *Neuroimage* **34**, 144-155, doi:10.1016/j.neuroimage.2006.09.018 (2007).

36 Hernandez-Fernandez, M. *et al.* Using GPUs to accelerate computational diffusion MRI: From microstructure estimation to tractography and connectomes. *Neuroimage* **188**, 598-615, doi:10.1016/j.neuroimage.2018.12.015 (2019).

37 Ma, L. *et al.* BAI-Net: Individualized Anatomical Cerebral Cartography Using Graph Neural Network. *IEEE Trans Neural Netw Learn Syst* **PP**, doi:10.1109/TNNLS.2022.3213581 (2022).

38 Wasserthal, J., Neher, P. & Maier-Hein, K. H. TractSeg - Fast and accurate white matter tract segmentation. *Neuroimage* **183**, 239-253, doi:10.1016/j.neuroimage.2018.07.070 (2018).

39 Paquola, C. *et al.* Microstructural and functional gradients are increasingly dissociated in transmodal cortices. *PLoS Biol* **17**, e3000284, doi:10.1371/journal.pbio.3000284 (2019).

40 Coifman, R. R. & Lafon, S. Diffusion maps. *Applied and computational harmonic analysis* **21**, 5-30 (2006).

41 Guell, X., Schmahmann, J. D., Gabrieli, J. & Ghosh, S. S. Functional gradients of the cerebellum. *Elife* **7**, doi:10.7554/eLife.36652 (2018).

42 Mesulam, M. M. in *Principles of behavioral and cognitive neurology, 2nd ed.* 1-120 (Oxford University Press, 2000).

43 von Economo, C. F., Koskinas, G. N. & Triarhou, L. C. *Atlas of cytoarchitectonics of the adult human cerebral cortex*. Vol. 10 (Karger Basel, 2008).

44 Paquola, C. *et al.* Shifts in myeloarchitecture characterise adolescent development of cortical gradients. *Elife* **8**, doi:10.7554/eLife.50482 (2019).

45 Karolis, V. R., Corbetta, M. & Thiebaut de Schotten, M. The architecture of functional lateralisation and its relationship to callosal connectivity in the human brain. *Nat Commun* **10**, 1417, doi:10.1038/s41467-019-09344-1 (2019).

46 Markello, R. D. *et al.* neuromaps: structural and functional interpretation of brain maps. *Nat Methods* **19**, 1472-1479, doi:10.1038/s41592-022-01625-w (2022).

47 Hansen, J. Y. *et al.* Mapping neurotransmitter systems to the structural and functional organization of the human neocortex. *Nat Neurosci* **25**, 1569-1581, doi:10.1038/s41593-022-01186-3 (2022).

48 Rosen, B. Q. & Halgren, E. An estimation of the absolute number of axons indicates that human cortical areas are sparsely connected. *PLoS Biol* **20**, e3001575, doi:10.1371/journal.pbio.3001575 (2022).

49 Neale, M. C. & Cardon, L. R.

50 Neale, M. C. *et al.* OpenMx 2.0: Extended Structural Equation and Statistical Modeling. *Psychometrika* **81**, 535-549, doi:10.1007/s11336-014-9435-8 (2016).

51 Markello, R. D. *et al.* Standardizing workflows in imaging transcriptomics with the abagen toolbox. *Elife* **10**, doi:10.7554/eLife.72129 (2021).

52 Arnatkeviciute, A., Fulcher, B. D. & Fornito, A. A practical guide to linking brain-wide gene expression and neuroimaging data. *Neuroimage* **189**, 353-367, doi:10.1016/j.neuroimage.2019.01.011 (2019).

53 Morgan, S. E. *et al.* Cortical patterning of abnormal morphometric similarity in psychosis is associated with brain expression of schizophrenia-related genes. *Proc Natl Acad Sci U S A* **116**, 9604-9609, doi:10.1073/pnas.1820754116 (2019).

54 Rakic, P., Ayoub, A. E., Breunig, J. J. & Dominguez, M. H. Decision by division: making cortical maps. *Trends Neurosci* **32**, 291-301, doi:10.1016/j.tins.2009.01.007 (2009).

55 Fjell, A. M. *et al.* Continuity and Discontinuity in Human Cortical Development and Change From Embryonic Stages to Old Age. *Cereb Cortex* **29**, 3879-3890, doi:10.1093/cercor/bhy266 (2019).

56 Yeo, B. T. *et al.* The organization of the human cerebral cortex estimated by intrinsic functional connectivity. *J Neurophysiol* **106**, 1125-1165, doi:10.1152/jn.00338.2011 (2011).

57 Adra, C. N. *et al.* Human ARHGDIG, a GDP-dissociation inhibitor for Rho proteins: genomic structure, sequence, expression analysis, and mapping to chromosome 16p13.3. *Genomics* **53**, 104-109, doi:10.1006/geno.1998.5482 (1998).

58 Arikkath, J. Molecular mechanisms of dendrite morphogenesis. *Front Cell Neurosci* **6**, 61, doi:10.3389/fncel.2012.00061 (2012).

59 Heyen, C. A., Tagliabracci, V. S., Zhai, L. & Roach, P. J. Characterization of mouse UDP-glucose pyrophosphatase, a Nudix hydrolase encoded by the Nudt14

gene. *Biochem Biophys Res Commun* **390**, 1414-1418, doi:10.1016/j.bbrc.2009.11.007 (2009).

60 Krenke, K. *et al.* FARSA mutations mimic phenylalanyl-tRNA synthetase deficiency caused by FARSB defects. *Clin Genet* **96**, 468-472, doi:10.1111/cge.13614 (2019).

61 Sansregret, L. & Nepveu, A. The multiple roles of CUX1: insights from mouse models and cell-based assays. *Gene* **412**, 84-94, doi:10.1016/j.gene.2008.01.017 (2008).

62 Yang, F. *et al.* Mouse SYCP2 is required for synaptonemal complex assembly and chromosomal synapsis during male meiosis. *J Cell Biol* **173**, 497-507, doi:10.1083/jcb.200603063 (2006).

63 Zhu, P. *et al.* A histone H2A deubiquitinase complex coordinating histone acetylation and H1 dissociation in transcriptional regulation. *Mol Cell* **27**, 609-621, doi:10.1016/j.molcel.2007.07.024 (2007).

64 Hendee, K. *et al.* Identification and functional analysis of an ADAMTSL1 variant associated with a complex phenotype including congenital glaucoma, craniofacial, and other systemic features in a three-generation human pedigree. *Hum Mutat* **38**, 1485-1490, doi:10.1002/humu.23299 (2017).

65 Lu, S. *et al.* Loss-of-function variants in TIAM1 are associated with developmental delay, intellectual disability, and seizures. *Am J Hum Genet* **109**, 571-586, doi:10.1016/j.ajhg.2022.01.020 (2022).

66 Ru, Q. *et al.* TIAM1-mediated synaptic plasticity underlies comorbid depression-like and ketamine antidepressant-like actions in chronic pain. *J Clin Invest* **132**, doi:10.1172/JCI158545 (2022).

67 Philp, D. J., Korgaonkar, M. S. & Grieve, S. M. Thalamic volume and thalamo-cortical white matter tracts correlate with motor and verbal memory performance. *Neuroimage* **91**, 77-83, doi:10.1016/j.neuroimage.2013.12.057 (2014).

68 Strick, P. L. The organization of thalamic inputs to the "premotor" areas. *Prog Brain Res* **64**, 99-109, doi:10.1016/S0079-6123(08)63405-6 (1986).

69 Janelle, F., Iorio-Morin, C., D'Amour, S. & Fortin, D. Superior Longitudinal

Fasciculus: A Review of the Anatomical Descriptions With Functional Correlates. *Front Neurol* **13**, 794618, doi:10.3389/fneur.2022.794618 (2022).

70 Koshiyama, D. *et al.* Association between the superior longitudinal fasciculus and perceptual organization and working memory: A diffusion tensor imaging study. *Neurosci Lett* **738**, 135349, doi:10.1016/j.neulet.2020.135349 (2020).

71 Takahashi, E., Folkerth, R. D., Galaburda, A. M. & Grant, P. E. Emerging cerebral connectivity in the human fetal brain: an MR tractography study. *Cereb Cortex* **22**, 455-464, doi:10.1093/cercor/bhr126 (2012).

72 Van Haastert, P. J. & Devreotes, P. N. Chemotaxis: signalling the way forward. *Nat Rev Mol Cell Biol* **5**, 626-634, doi:10.1038/nrm1435 (2004).

73 Wu, D. Signaling mechanisms for regulation of chemotaxis. *Cell Res* **15**, 52-56, doi:10.1038/sj.cr.7290265 (2005).

74 Kast, R. J. & Levitt, P. Precision in the development of neocortical architecture: From progenitors to cortical networks. *Prog Neurobiol* **175**, 77-95, doi:10.1016/j.pneurobio.2019.01.003 (2019).

75 Langen, M. *et al.* The Developmental Rules of Neural Superposition in Drosophila. *Cell* **162**, 120-133, doi:10.1016/j.cell.2015.05.055 (2015).

76 Sansom, S. N. & Livesey, F. J. Gradients in the brain: the control of the development of form and function in the cerebral cortex. *Cold Spring Harb Perspect Biol* **1**, a002519, doi:10.1101/cshperspect.a002519 (2009).

77 Valk, S. L. *et al.* Shaping brain structure: Genetic and phylogenetic axes of macroscale organization of cortical thickness. *Sci Adv* **6**, doi:10.1126/sciadv.abb3417 (2020).

78 Yang, S. *et al.* Cortical patterning of morphometric similarity gradient reveals diverged hierarchical organization in sensory-motor cortices. *Cell Rep* **36**, 109582, doi:10.1016/j.celrep.2021.109582 (2021).

79 Flores-Sarnat, L. & Sarnat, H. B. Axes and gradients of the neural tube for a morphological/molecular genetic classification of nervous system malformations. *Handb Clin Neurol* **87**, 1-11, doi:10.1016/S0072-9752(07)87001-1 (2008).

80 Hoch, R. V., Rubenstein, J. L. & Pleasure, S. Genes and signaling events that

establish regional patterning of the mammalian forebrain. *Semin Cell Dev Biol* **20**, 378-386, doi:10.1016/j.semcdb.2009.02.005 (2009).

81 Storm, E. E. *et al.* Dose-dependent functions of Fgf8 in regulating telencephalic patterning centers. *Development* **133**, 1831-1844, doi:10.1242/dev.02324 (2006).

82 Sun, T. & Hevner, R. F. Growth and folding of the mammalian cerebral cortex: from molecules to malformations. *Nat Rev Neurosci* **15**, 217-232, doi:10.1038/nrn3707 (2014).

83 Hamasaki, T., Leingartner, A., Ringstedt, T. & O'Leary, D. D. EMX2 regulates sizes and positioning of the primary sensory and motor areas in neocortex by direct specification of cortical progenitors. *Neuron* **43**, 359-372, doi:10.1016/j.neuron.2004.07.016 (2004).

84 Bolz, J. *et al.* Multiple roles of ephrins during the formation of thalamocortical projections: maps and more. *J Neurobiol* **59**, 82-94, doi:10.1002/neu.10346 (2004).

85 Gao, P. P. *et al.* Regulation of thalamic neurite outgrowth by the Eph ligand ephrin-A5: implications in the development of thalamocortical projections. *Proc Natl Acad Sci U S A* **95**, 5329-5334, doi:10.1073/pnas.95.9.5329 (1998).

86 Fenlon, L. R., Suarez, R. & Richards, L. J. The anatomy, organisation and development of contralateral callosal projections of the mouse somatosensory cortex. *Brain Neurosci Adv* **1**, 2398212817694888, doi:10.1177/2398212817694888 (2017).

87 Barone, P., Dehay, C., Berland, M. & Kennedy, H. Role of directed growth and target selection in the formation of cortical pathways: prenatal development of the projection of area V2 to area V4 in the monkey. *J Comp Neurol* **374**, 1-20, doi:10.1002/(SICI)1096-9861(19961007)374:1<1::AID-CNE1>3.0.CO;2-7 (1996).

88 Casingal, C. R., Descant, K. D. & Anton, E. S. Coordinating cerebral cortical construction and connectivity: Unifying influence of radial progenitors. *Neuron* **110**, 1100-1115, doi:10.1016/j.neuron.2022.01.034 (2022).

89 Nowakowski, T. J., Pollen, A. A., Sandoval-Espinosa, C. & Kriegstein, A. R. Transformation of the Radial Glia Scaffold Demarcates Two Stages of Human Cerebral Cortex Development. *Neuron* **91**, 1219-1227, doi:10.1016/j.neuron.2016.09.005 (2016).

90 Marsoner, F., Koch, P. & Ladewig, J. Cortical organoids: why all this hype? *Curr Opin Genet Dev* **52**, 22-28, doi:10.1016/j.gde.2018.04.008 (2018).

91 Quadrato, G. & Arlotta, P. Present and future of modeling human brain development in 3D organoids. *Curr Opin Cell Biol* **49**, 47-52, doi:10.1016/j.ceb.2017.11.010 (2017).

92 Giaccio, R. G. The dual origin hypothesis: an evolutionary brain-behavior framework for analyzing psychiatric disorders. *Neurosci Biobehav Rev* **30**, 526-550, doi:10.1016/j.neubiorev.2005.04.021 (2006).

93 Pandya, D., Seltzer, B., Petrides, M. & Cipolloni, P. B. *Cerebral Cortex: Architecture, Connections, and the Dual Origin Concept*. (Oxford University Press, 2015).

94 Pandya, D. N. & Seltzer, B. Intrinsic connections and architectonics of posterior parietal cortex in the rhesus monkey. *J Comp Neurol* **204**, 196-210, doi:10.1002/cne.902040208 (1982).

95 Pandya, D. N., Seltzer, B. & Barbas, H. Input-output organization of the primate cerebral cortex. (1986).

96 Petrides, M. & Pandya, D. N. Dorsolateral prefrontal cortex: comparative cytoarchitectonic analysis in the human and the macaque brain and corticocortical connection patterns. *Eur J Neurosci* **11**, 1011-1036, doi:10.1046/j.1460-9568.1999.00518.x (1999).

97 Petrides, M. & Pandya, D. N. Comparative cytoarchitectonic analysis of the human and the macaque ventrolateral prefrontal cortex and corticocortical connection patterns in the monkey. *Eur J Neurosci* **16**, 291-310, doi:10.1046/j.1460-9568.2001.02090.x (2002).

98 Lariviere, S. *et al.* Multiscale Structure-Function Gradients in the Neonatal Connectome. *Cereb Cortex* **30**, 47-58, doi:10.1093/cercor/bhz069 (2020).

99 Dong, H. M., Margulies, D. S., Zuo, X. N. & Holmes, A. J. Shifting gradients of macroscale cortical organization mark the transition from childhood to adolescence. *Proc Natl Acad Sci U S A* **118**, doi:10.1073/pnas.2024448118 (2021).

100 Huttenlocher, P. R. Synaptic density in human frontal cortex - developmental

changes and effects of aging. *Brain Res* **163**, 195-205, doi:10.1016/0006-8993(79)90349-4 (1979).

101 Huttenlocher, P. R., De Courten, C., Garey, L. J. & Van der Loos, H. Synaptic development in human cerebral cortex. *Int J Neurol* **16-17**, 144-154 (1982).

102 Ito, T. & Murray, J. D. Multitask representations in the human cortex transform along a sensory-to-motor hierarchy. *Nat Neurosci*, doi:10.1038/s41593-022-01224-0 (2022).

103 Auladell, C., Perez-Sust, P., Super, H. & Soriano, E. The early development of thalamocortical and corticothalamic projections in the mouse. *Anat Embryol (Berl)* **201**, 169-179, doi:10.1007/pl00008238 (2000).

104 Hohl-Abrahao, J. C. & Creutzfeldt, O. D. Topographical mapping of the thalamocortical projections in rodents and comparison with that in primates. *Exp Brain Res* **87**, 283-294, doi:10.1007/BF00231845 (1991).

105 Olivares, R., Montiel, J. & Aboitiz, F. Species differences and similarities in the fine structure of the mammalian corpus callosum. *Brain Behav Evol* **57**, 98-105, doi:10.1159/000047229 (2001).

106 Velut, S., Destrieux, C. & Kakou, M. [Morphologic anatomy of the corpus callosum]. *Neurochirurgie* **44**, 17-30 (1998).

107 Mahjoory, K., Schoffelen, J. M., Keitel, A. & Gross, J. The frequency gradient of human resting-state brain oscillations follows cortical hierarchies. *Elife* **9**, doi:10.7554/eLife.53715 (2020).

108 Hillebrand, A. *et al.* Direction of information flow in large-scale resting-state networks is frequency-dependent. *Proc Natl Acad Sci U S A* **113**, 3867-3872, doi:10.1073/pnas.1515657113 (2016).

109 Keitel, A. & Gross, J. Individual Human Brain Areas Can Be Identified from Their Characteristic Spectral Activation Fingerprints. *PLoS Biol* **14**, e1002498, doi:10.1371/journal.pbio.1002498 (2016).

110 Mellem, M. S., Wohltjen, S., Gotts, S. J., Ghuman, A. S. & Martin, A. Intrinsic frequency biases and profiles across human cortex. *J Neurophysiol* **118**, 2853-2864, doi:10.1152/jn.00061.2017 (2017).

111 Mueller, S. *et al.* Individual variability in functional connectivity architecture of the human brain. *Neuron* **77**, 586-595, doi:10.1016/j.neuron.2012.12.028 (2013).

112 Powell, A. W., Sassa, T., Wu, Y., Tessier-Lavigne, M. & Polleux, F. Topography of thalamic projections requires attractive and repulsive functions of Netrin-1 in the ventral telencephalon. *PLoS Biol* **6**, e116, doi:10.1371/journal.pbio.0060116 (2008).

113 Vanderhaeghen, P. & Polleux, F. Developmental mechanisms patterning thalamocortical projections: intrinsic, extrinsic and in between. *Trends Neurosci* **27**, 384-391, doi:10.1016/j.tins.2004.05.009 (2004).

114 Maier-Hein, K. H. *et al.* The challenge of mapping the human connectome based on diffusion tractography. *Nat Commun* **8**, 1349, doi:10.1038/s41467-017-01285-x (2017).

115 Reveley, C. *et al.* Superficial white matter fiber systems impede detection of long-range cortical connections in diffusion MR tractography. *Proc Natl Acad Sci U S A* **112**, E2820-2828, doi:10.1073/pnas.1418198112 (2015).

116 Axer, M. & Amunts, K. Scale matters: The nested human connectome. *Science* **378**, 500-504, doi:10.1126/science.abq2599 (2022).

117 Howard, A. F. *et al.* The BigMac dataset: an open resource combining multi-contrast MRI and microscopy in the macaque brain. *bioRxiv* (2022).

118 Huang, S. Y. *et al.* Connectome 2.0: Developing the next-generation ultra-high gradient strength human MRI scanner for bridging studies of the micro-, meso- and macro-connectome. *Neuroimage* **243**, 118530, doi:10.1016/j.neuroimage.2021.118530 (2021).

119 Harris, J. A. *et al.* Hierarchical organization of cortical and thalamic connectivity. *Nature* **575**, 195-202, doi:10.1038/s41586-019-1716-z (2019).

120 Axer, M. *et al.* A novel approach to the human connectome: ultra-high resolution mapping of fiber tracts in the brain. *Neuroimage* **54**, 1091-1101, doi:10.1016/j.neuroimage.2010.08.075 (2011).

121 Wang, H. *et al.* as-PSOCT: Volumetric microscopic imaging of human brain architecture and connectivity. *Neuroimage* **165**, 56-68, doi:10.1016/j.neuroimage.2017.10.012 (2018).

122 Pang, J. C. *et al.* Geometric constraints on human brain function. *Nature*, doi:10.1038/s41586-023-06098-1 (2023).

123 Gordon, E. M. *et al.* Generation and Evaluation of a Cortical Area Parcellation from Resting-State Correlations. *Cereb Cortex* **26**, 288-303, doi:10.1093/cercor/bhu239 (2016).

124 Miura, Y. *et al.* Engineering brain assembloids to interrogate human neural circuits. *Nat Protoc* **17**, 15-35, doi:10.1038/s41596-021-00632-z (2022).

125 Sloan, S. A., Andersen, J., Pasca, A. M., Birey, F. & Pasca, S. P. Generation and assembly of human brain region-specific three-dimensional cultures. *Nat Protoc* **13**, 2062-2085, doi:10.1038/s41596-018-0032-7 (2018).